REPORT DOCUMENTATION PAGE

Form Approved
OMB No. 0704-0188

PLEASE DO NOT RETURN YOUR FORM TO THE ABOVE ADDRESS.

1. REPORT DATE *(DD-MM-YYYY)*	2. REPORT TYPE	3. DATES COVERED *(From - To)*
07-05-2012		

4. TITLE AND SUBTITLE

Direct Writing of Graphene-based Nanoelectronics via Atomic Force Microscopy

5a. CONTRACT NUMBER

5b. GRANT NUMBER

5c. PROGRAM ELEMENT NUMBER

6. AUTHOR(S)

Haydell, Michael Wayne Jr.

5d. PROJECT NUMBER

5e. TASK NUMBER

5f. WORK UNIT NUMBER

7. PERFORMING ORGANIZATION NAME(S) AND ADDRESS(ES)

8. PERFORMING ORGANIZATION REPORT NUMBER

9. SPONSORING/MONITORING AGENCY NAME(S) AND ADDRESS(ES)

U.S. Naval Academy
Annapolis, MD 21402

10. SPONSOR/MONITOR'S ACRONYM(S)

11. SPONSOR/MONITOR'S REPORT NUMBER(S)

Trident Scholar Report no. 405 (2012)

12. DISTRIBUTION/AVAILABILITY STATEMENT

This document has been approved for public release; its distribution is UNLIMITED

13. SUPPLEMENTARY NOTES

14. ABSTRACT

This project employs direct writing with an atomic force microscope (AFM) to fabricate simple graphene-based electronic components like resistors and transistors at nanometer-length scales. The goal is to explore their electrical properties for graphene-based electronics. Conducting nanoribbons of graphene were fabricated using thermochemical nanolithography (TCNL). TCNL uses a heated AFM cantilever to provide precise local heating to an insulating fluorographene (FG) substrate. The heat reduces the substrate into a material known as reduced fluorographene (rFG), which exhibits electric properties similar to those of pristine graphene. Compared to other attempts to produce graphene-based devices, this technique is simple, does not involve solvents or other complicated fabrication steps, and allows for the exact placement of the devices on the wafer.

15. SUBJECT TERMS

graphene, nanolithography, atomic force microscope, transistors

16. SECURITY CLASSIFICATION OF:			17. LIMITATION OF ABSTRACT	18. NUMBER OF PAGES	19a. NAME OF RESPONSIBLE PERSON
a. REPORT	b. ABSTRACT	c. THIS PAGE		64	19b. TELEPHONE NUMBER *(Include area code)*

A TRIDENT SCHOLAR PROJECT REPORT

NO. 405

Direct Writing of Graphene-based Nanoelectronics via Atomic Force Microscopy

by

Midshipman 1/C Michael W. Haydell Jr, USN

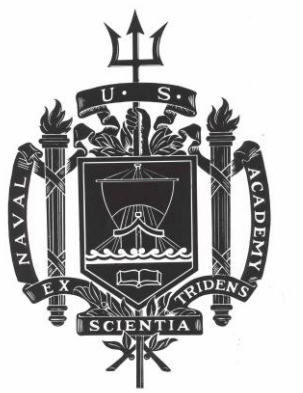

UNITED STATES NAVAL ACADEMY
ANNAPOLIS, MARYLAND

U.S.N.A. --- Trident Scholar project report; no. 405 (2012)

Direct Writing of Graphene-based Nanoelectronics via Atomic Force Microscopy

by

Midshipman 1/C Michael W. Haydell Jr.
United States Naval Academy
Annapolis, Maryland

_____
(signature)

Certification of Adviser(s) Approval

Assistant Professor Elena Cimpoiasu
Physics Department

_____
(signature)

_____
(date)

Dr. Paul E. Sheehan
Naval Research Laboratory

_____
(signature)

_____
(date)

Acceptance for the Trident Scholar Committee

Professor Carl E. Wick
Associate Director of Midshipman Research

_____
(signature)

_____
(date)

USNA-1531-2

ABSTRACT

This Trident project employs direct writing with an atomic force microscope (AFM) to fabricate simple graphene-based electronic components like resistors and transistors at nanometer-length scales. The goal is to explore their electronic properties and the feasibility of using this technique for the manufacturing of graphene-based electronics. The graphene devices are expected to be denser and faster, and to dissipate heat more efficiently than current silicon-based transistors. Here we fabricate conducting nanoribbons of graphene using two different AFM techniques, thermochemical nanolithography (TCNL) and thermal dip-pen nanolithography (tDPN). TCNL involves flowing current through an AFM tip to provide precise local heating to an insulating graphene substrate (graphene oxide or graphene fluoride). The heat reduces the substrate into a material known as reduced graphene oxide/fluoride (rGO/F) which exhibits electric properties close to those of pristine graphene. These nanoribbons can be used to fabricate nanoscale electronic components such as resistors, capacitors, and transistors. Compared to other attempts to produce graphene-based devices, this technique is simple, does not involve solvents or other complicated fabrication steps, and allows for the exact placement of the devices on the wafer. The thermal dip pen nanolithography uses a heated AFM tip dipped in polymer which leaves a layer of masking material on the surface of pristine graphene. When the

graphene sheet is functionalized through fluorination and thereby rendered insulating, the narrow layer of polymer locally protects the graphene underneath. The properties of the devices produced using these two fabrication methods are compared by measuring their electrical current-voltage characteristics.

Keywords: MOSFET Circuits, Nanoelectronics, Graphene Transistors, Thermochemical Nanolithography

ACKNOWLEDGMENTS

I would like to thank my advisors, Dr. Elena Cimpoiasu and Dr. Paul Sheehan, for leading me through this Trident project. Without their patience and guidance, I would not have succeeded. Furthermore, Dr. Woo Kyung Lee deserves full credit for taking me under his wing and teaching me everything I know about thermochemical nanolithography, atomic force microscopy, and nanoscience research. I must also thank the Naval Research Laboratory for allowing me access onto the facility and use of their assets. Professor Wick and the Trident Committee also deserve my appreciation for accepting me to the ranks of the Trident Scholars and authorizing the funding for the research. Behind the scenes were Ms. Joan Beall and Ms. Irene Starr who helped me to travel from the Naval Academy, to the lab, and back. They made the travel easy for me so I did not have to worry about this very important logistical hurdle. Finally, I must thank my parents for the infinite hours they spent supporting me through both the hard times, and the easy. They served as my rock, on which I built this experience.

“The principles of physics, as far as I can see, do not speak against the possibility of maneuvering things atom by atom. It is not an attempt to violate any laws; it is something, in principle, that can be done; but in practice, it has not been done because we are too big.”

-Richard P. Feynman (29 December, 1959)

TABLE OF CONTENTS

1. Introduction

1.1 Background and Motivation

1.2 Graphene: The Wonder Material

1.3 Functionalized Graphene

1.4 Atomic Force Microscopy

1.5 Thermochemical Nanolithography

1.6 MOSFET Transistors

2. Other Methods to Fabricate Graphene-Based Transistors

2.1 Photolithography

2.2 Thermochemical Nanolithography of Graphene Oxide

2.3 Thermal Dip-Pen Nanolithography

3. Experiment: Thermochemical Nanolithography of Fluorographene

3.1 Sample Fabrication

3.2 Functionalization: Forming Fluorographene

3.3 Reduction

3.4 Challenges

4. Characterization

4.1 Physical Characterization

4.2 Electrical Characterization

4.3 Sheet Resistance

5. Effects of Changing Reduction Variables

5.1 Changing the Tip Temperature

5.2 Changing the Writing Speed

5.3 Effect of Forming Gas

6. Comparison to Other Methods

6.1 TCNL versus Photolithography

6.2 TCNL of Fluorographene versus TCNL of Graphene Oxide

6.3 TCNL of Fluorographene versus tDPN

7. Conclusion

References

Appendix A: Step-by-Step process

LIST OF FIGURES

Figure 1: Graph of Moore's Law 9
Figure 2: Graphic representation of graphene 10
Figure 3: Graphic explaining band gaps 12
Figure 4: Fluorographene 13
Figure 5: Atomic force microscope used in the roject 14
Figure 6: How an AFM works 15
Figure 7: AFM height image of graphene oxide flakes on Si 15
Figure 8: AFM friction image of flake in Fig 7 15
Figure 9: Heatable cantilever 16
Figure 10: The electrodes of a MOSFET and the fields they create 17
Figure 11: MOSFET in off state 18
Figure 12: MOSFET in triode state 18
Figure 13: MOSFET in saturation mode 19
Figure 14: IV curve at various V_{GS} for MOSFET operation 19
Figure 15: Illustration of the photolithography process 20
Figure 16: Effect of exposure on photoresist 22
Figure 17: Illustration of the TCNL process 23
Figure 18: Effect of temperature on reduction of graphene oxide 24
Figure 19: Polymer deposit onto surface from heated tip 25
Figure 20: Illustration of thermal dip-pen nanolithography 26
Figure 21: Electrodes arranged on sample 28
Figure 22: IV curve for an open circuit device 29
Figure 23: Graphene samples before and after reduction 30
Figure 24: Tip skipping off of gold electrode 32
Figure 25: Tip holder adapter design by author and AFM tip 33
Figure 26: Section image across device in Figure 23 35
Figure 27: Friction image of device in Figure 23 36
Figure 28: Friction image after flattening 36
Figure 29: 3D height image of rFG nanoribbon 37
Figure 30: Section across rFG nanoribbons 37
Figure 31: How measurements were made 38

Figure 32: Probe station where measurements are made 39
Figure 33: Electrical characterization of the device in Figure 23 40
Figure 34: Observed field effect of Figure 23 device 41
Figure 35: Transconductivity measurement of Figure 23 device 42
Figure 36: Explanation for importance of sheet resistance 43
Figure 37: Variable temperature test 46
Figure 38: Results from the variable temperature test 47
Figure 39: Height image from variable speed test 49
Figure 40: Friction image from variable speed test 49
Figure 41: Height section images for variable speed test 50
Figure 42: Friction section images for variable speed test 51
Figure 43: Nanoribbons written in forming gas 52
Figure 44: Effect of forming gas on reduction 53
Figure 45: Reduction is more reliable in forming gas 54
Figure 46: Writing speed vs. LFM signal variation under forming gas 55
Figure 47: Writing speed vs. device sheet resistance under forming gas 55
Figure 48: Cartoon image of ideal rFG transistor 58

CHAPTER 1: INTRODUCTION

1.1 Background and Motivation

In the wake of scientific advances, new and sophisticated technologies arise. This effect is nowhere more obvious than in the field of computer electronics and information technology. The strong relation between research and technology has allowed for tremendous advances in these fields. Most impressively, the density of the electronic components packed on a processor chip has doubled every two years. This trend, known as Moore's law, has held true for the last half century, as shown in Figure 1.

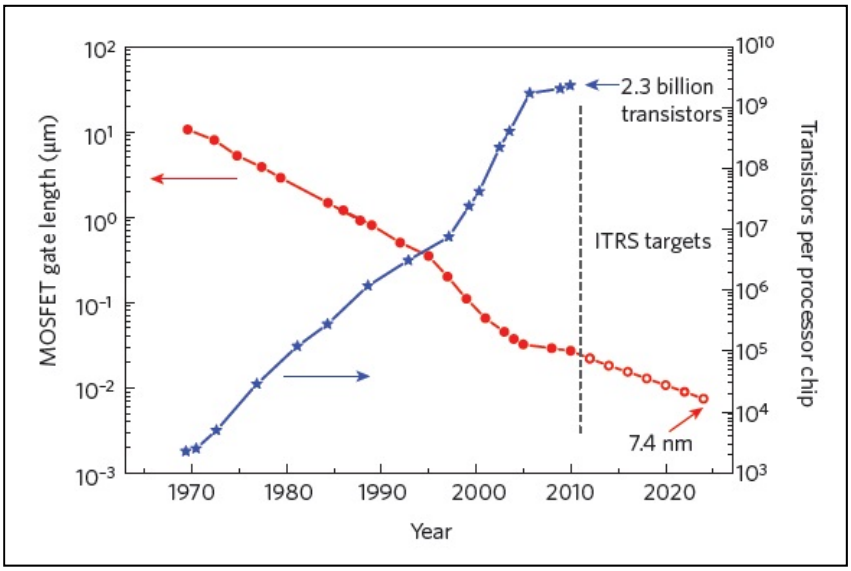

Fig 1: Graph of Moore's law [1]

Unfortunately, a critical threshold will soon be reached and Moore's law will no longer apply. A transistor cannot be made smaller than the size of an atom, the basic building block of matter. However, as devices shrink, many hurdles need to be overcome. For instance, heat transfer becomes a limiting factor as the heat generated can actually melt the processors. Also, as the density increases, the negative effects of fabrication defects increase as well. From a financial perspective, using current methodologies to make better and smaller transistors will become prohibitively expensive as the equipment used in the clean room needs to be improved. Not only are multiple machines required in the current fabrication process, but each machine is very complex, requiring an enormous investment and years of training to use.

A processor in a modern computer contains approximately 2 billion transistors, each about 30 nm long [1]. In order to shrink these devices and overcome the hurdles associated with that goal, new materials and methods will be needed to replace the traditional silicon technologies. This Trident project addresses these issues through the fabrication and testing of nano-scale electronic components using both a new material and a new fabrication process.

1.2 Graphene: The Wonder Material

Graphene (Figure 2) has the potential to overcome many of the difficulties associated with improving transistor performance. Because of its interesting properties, graphene has attracted much attention in the research community since it was first isolated by Dr. Andre Geim in 2004

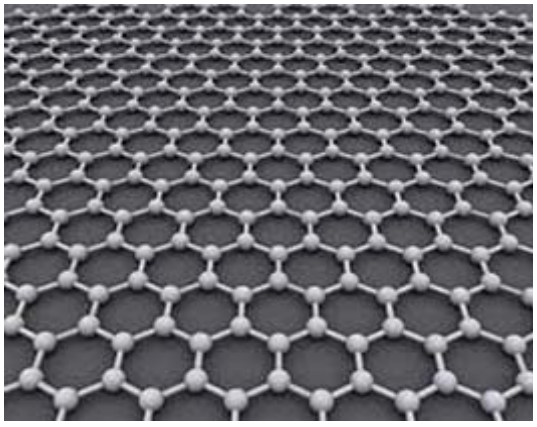

Fig 2: Graphic representation of graphene [3]

[2]. This was accomplished by mechanical exfoliation, by using tape to peel off thin pieces of graphite that would then be smeared across a silicon substrate with the hope that a single sheet of graphite, known as graphene, would be transferred. This wonder material is a two-dimensional array of carbon atoms arranged in a hexagonal pattern, reminiscent of chicken wire. The type of bond that the carbon atoms form in graphene is classified as sp^2, which cause the sheet to lie flat, therefore making it two dimensional. The distance between each atom is 1.42 Å, and the lattice constant is 2.46 Å [1]. It is also one of the stiffest materials known to humans [4].

The properties that make graphene important for the computer industry are its thermal conductivity and electrical properties. Graphene has the highest known thermal conductivity [5], which allows heat to be transferred away from electronic devices more effectively compared to silicon, meaning that transistors could be more densely packed without fear of thermal damage. Electrically, graphene has a zero band gap, making it a semimetal. Electrical charges in graphene can also have exceedingly high electron mobilities [6], a measure of how well an electron can travel through a material. High mobility means that the electrons can travel almost unimpeded through the material, allowing for the transistors to switch on or off more quickly than is possible in today's computers. Depending on the type of graphene and its quality, mobilities can range from 1000 to 1,000,000 $cm^2\ V^{-1}\ s^{-1}$ [1]. Compare this value to silicon's, which is 450 $cm^2\ V^{-1}\ s^{-1}$ [7].

Currently, there are three approaches for preparing graphene: mechanical exfoliation, chemical vapor deposition, and thermal decomposition of SiC [1]. Exfoliation techniques are interesting from a research perspective but do not produce samples large enough to be useful in the electronics industry. The other options, however, can produce graphene on a wafer scale. Chemical vapor deposition (CVD) uses heat to decompose a carbon-rich material as a source of

carbon. The atoms then arrange into sp^2 carbon using a catalyst, usually a metal [8]. Therefore, CVD grows graphene on a thin metal film, and the graphene can subsequently be transferred to an insulating substrate. CVD grown graphene is regularly single layer when used with our choice of metal, copper. Epitaxial graphene involves the thermal decomposition of SiC. This method is fairly clean as the support crystal, hexagonal α-SiC, provides the carbon and already matches the geometry. Also, no metal is involved [8]. However, the epitaxial process is not self-limiting, which means epitaxial graphene is usually several layers thick, and this added thickness can complicate the reduction process. Furthermore, the high cost of SiC substrates would preclude many applications.

1.3 Functionalized Graphene

The electric properties of a material depend on the material's band structure. The band gap of a material determines how well a material conducts electrons. The band gap is the difference in energy between the valence band, or the outermost electron shell of an atom, and the conduction band, the area where electrons can flow more or less freely. The larger the band gap, the more energy is required to move electrons from the valence band to the conduction band. Metals conduct electrons well because the conduction band overlaps the valence band,

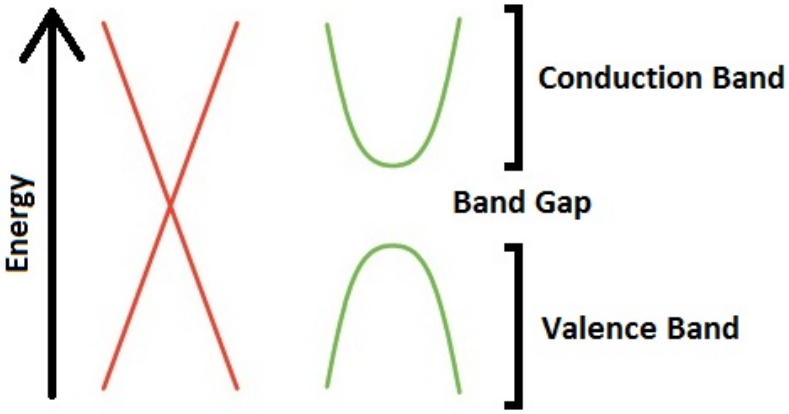

Fig 3: Zero band gap (Red), Opened band gap (Green) [1]

while insulators impede electron transport because they have a large gap.

Graphene has a zero band gap. This means the valence band and conduction band are touching, as in the red cones in Figure 3. An interesting feature of graphene's 0 eV band gap is that is can be opened, making it semiconducting (green curves in Figure 3). For a transistor to work, the material needs to demonstrate a field effect, the phenomenon that applying a transverse electric field across a material modulates how easily a current flows through a biased channel in that material. A metal or semimetal will not exhibit a field effect. Semiconductors, however, do.

Graphene's band gap can be opened in two ways, physical confinement or chemical functionalization [8]. Confinement refers to shaping the graphene into small structures. One way is to carve nanoribbons from a larger graphene sheet. The resulting ribbon is rectangular with quasi-one-dimensional topology; namely, the length is much greater than the width. It has been suggested graphene's band gap is inversely proportional to the ribbon width. Unfortunately, shaping sufficiently narrow ribbons (<10 nm) creates rough edges which negatively impact the electric properties [1]. Chemical functionalization involves attaching other elements onto the carbon surface, therefore opening the band gap and changing the current carrying capacity of graphene without introducing rough edges [6].

Graphene Oxide (GO) is simply a sheet of graphene that has oxygen-rich functional groups attached on one side. Oxidizing graphene changes the current carrying properties enough that the material becomes insulating with a band gap of .5 eV. A material similar to GO can be created by fluorinating, as opposed to oxidizing, graphene. Fluorographene (FG) has one fluorine atom per four carbons (Figure 4) which opens a band gap

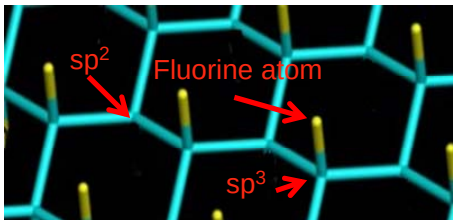

Fig 4: Fluorographene (C_4F) [10]

of 2.93 eV and both FG and GO can be reduced back into the semiconducting graphene [6,9]. When functionalized, the bonds between the carbon atoms and the functionalizing atoms are classified as sp^3. The sp^3 bonds cause ripples in the functionalized form of the graphene. It can still be considered two dimensional because the material is "all surface."

1.4 Atomic Force Microscopy

In 1985 [11], Binnig, Quate, and Gerber, invented the atomic force microscope (AFM). A common AFM is shown in Figure 5. An AFM images a surface using a small moving probe that travels over the surface being imaged. As the probe scans the material, it will move up or down with nanometer resolution to follow the topography of the surface. To sense these small up and down motions, a laser beam reflects off the vibrating tip into a detector. As the tip moves, the position of the laser beam in the detector will move [13]. Therefore, this detector is how the microscope "sees" the imaged object. Using this technique, the instrument can resolve changes in height and position with an accuracy of fractions of a nanometer. "Contact microscopy" is commonly used to image objects smaller than 500 nanometers, as one cannot conventionally use optics to image samples smaller than the wavelength of light. Figure 6 provides an illustration of the AFM imaging process. Figure 7

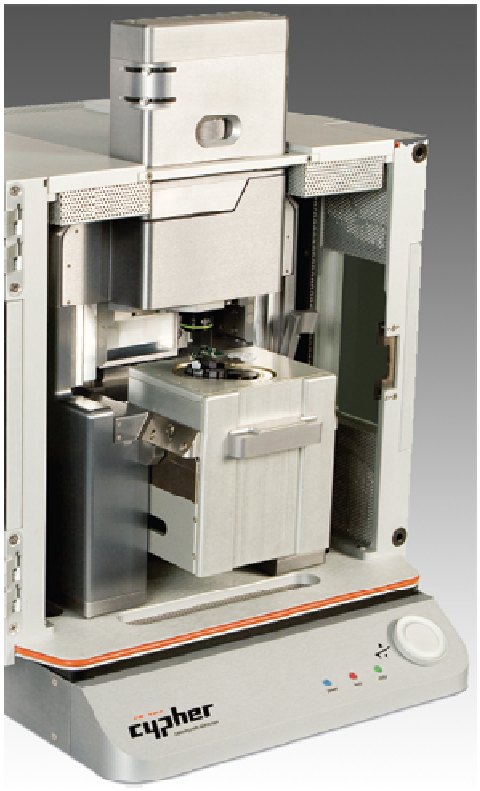

Fig 5: Atomic force microscope used in the project [12]

shows an AFM "height image," where the convention is that the lighter areas are topographically higher than the darker areas.

Atomic force microscopes are convenient because they can operate at room temperature, in air, and can image almost any surface [13]. They can also distinguish surfaces with different friction coefficients. This is because as the tip travels along the surface, areas of high friction twist the tip causing the beam to shift sideways in the detector. An AFM can use the difference in friction to create a different picture of the image. Areas of high friction will appear different from areas of low friction, which allows someone to distinguish one material from another. Figure 8 is a lateral force microscopy image, or AFM friction mode, of the same flakes in Figure 7. Figure 8 shows the contrast between areas of high friction and areas of low friction, known as the friction force variation, expressed in mV.

Beyond imaging, AFMs can use the probe to manipulate or change a surface. For example, one can use the tip to indent the surface, scratch

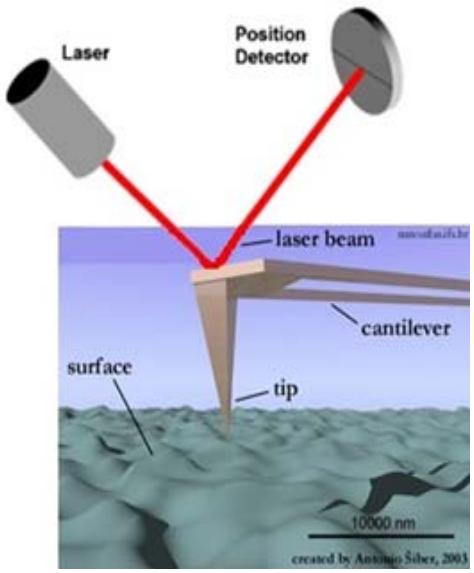

Fig 6: How an AFM works [14]

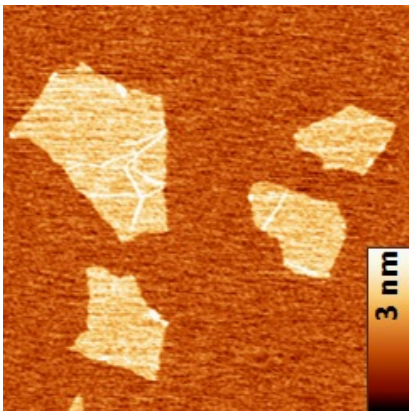

Fig 7: AFM height image of GO flakes on Si [5]

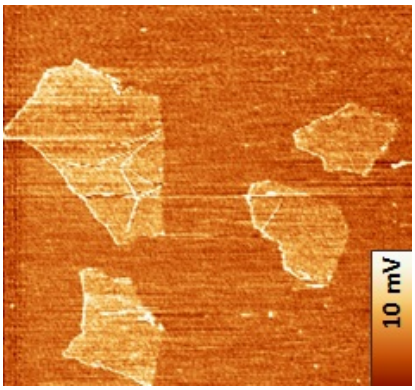

Fig 8: AFM friction image of flakes in Fig 7 [5]

patterns into the surface, cut samples, or push small features. Indeed, because of the high positioning capability of scanning probes, it is possible to perform lithography atom by atom [15], the ultimate limit in lithography. As the scanning probe can be used in many different modes, there are many different lithography techniques. For instance, thermochemical nanolithography and thermal dip-pen nanolithography are two methods explored in this research.

1.5 Thermochemical Nanolithography

Unfortunately, graphene is not as easily fabricated as is silicon. From an engineering standpoint, the extra complication drives up production cost offsetting the benefits that graphene can provide. Therefore, a method to cheaply, quickly, and easily fabricate transistors needs to be explored to keep the cost of a graphene computer economical.

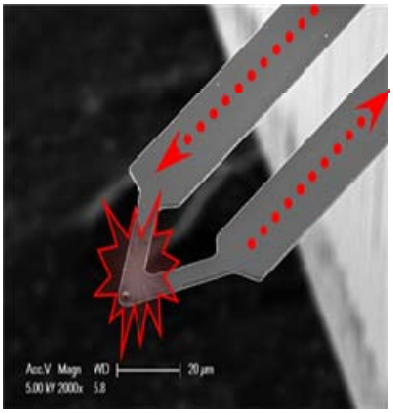

Fig 9: Heatable cantilever. Current flows through the legs and resistively heats the area under the tip, the small bump at the end of the legs [5]

The primary goal of this Trident project was to explore the possibility of using an atomic force microscopy technique called thermochemical nanolithography (TCNL) as a method to write transistors into a fluorographene sheet. The idea is to make the ribbon sufficiently small so that it has a band gap, but there will be no edge effects because the graphene sheet is preserved, so the mobility is recovered. Ideally there should be no fluorine left in the ribbon, but some residual fluorine will remain.

TCNL uses an AFM cantilever, shown in Figure 9, heated by flowing a current through the tip, to locally heat the sample. The tip can be heated to 1000℃ in only a few microseconds.

In TCNL, one locally converts a non-conducting film to a conducting state. This is achieved by adding thermal energy to the functionalized graphene substrate to locally reduce the FG back into graphene.

This method allows one to directly write electronic circuits. Different geometries can be created by translating the tip over the graphene surface. For example, a transistor is made by drawing a line bridging two electrodes. The major advantage of thermochemical nanolithography is single-step fabrication. It can also produce devices with widths as small as 12 nm [6]. In principle, TCNL can be used to quickly, cheaply, and efficiently write graphene-based devices with nanometer resolution.

1.6 MOSFET Transistors

A transistor is simply a switch that can be turned either on or off. These states can be made to arbitrarily represent either a 1 or 0, which are the only two characters of binary code, the language of computers. A computer needs millions or billions of transistors to perform useful functions, which is why the manufacturing process needs to be efficient, but the operation of a metal oxide semiconductor field effect transistor (MOSFET) is fairly simple.

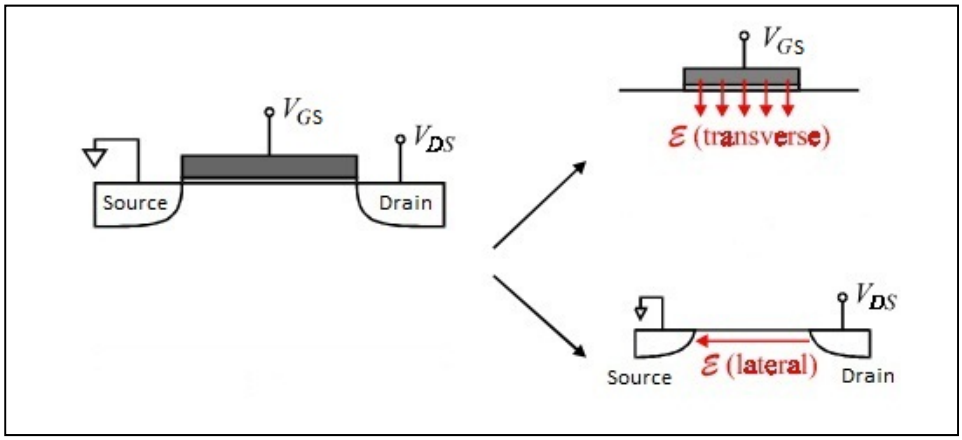

Fig 10: The electrodes of a MOSFET and the fields they create [16]

Typically a MOSFET consists of three electrodes (source, drain, and gate) connecting a semiconducting channel to external electronics (Figure 10). The gate electrode is biased compared to the source electrode by V_{GS}, which generates a transverse electric field that permeates the semiconducting material and concentrates charge carriers towards the surface [16]. The potential needed to displace these electrons is called the threshold voltage, V_T. The displaced electrons will move between the source and drain electrodes under the effect of a lateral electric field if the drain electrode is biased by V_{DS}. Below V_T the device is off, or in the 0 state, as in Figure 11.

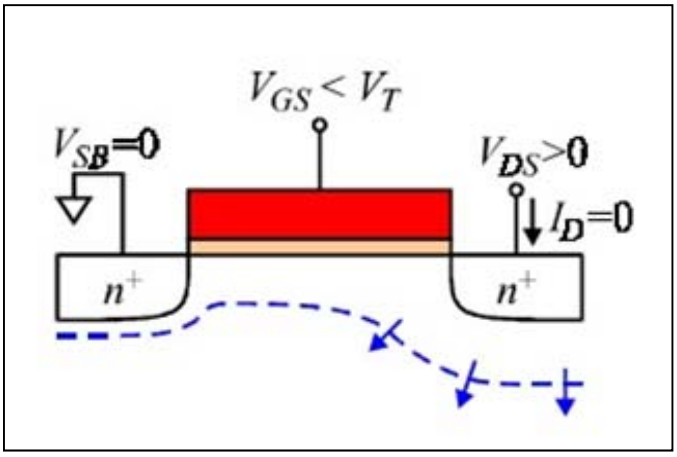

Fig 11: MOSFET in off state [16]

The source and drain electrodes provide a lateral potential, V_{DS}, to push electrons across the channel causing an on, or 1, state. If the fully conductive graphene was used, the transistor would always be closed. This is why graphene's 0 eV band gap needs to be opened for application, hence the necessity of chemical functionalization. The reduced fluorographene is a semiconductor that enables control over the concentration of the free carriers, allowing the transistor to be turned off. In this state, known as triode operation, increasing either the gate potential or the drain-source potential will increase the

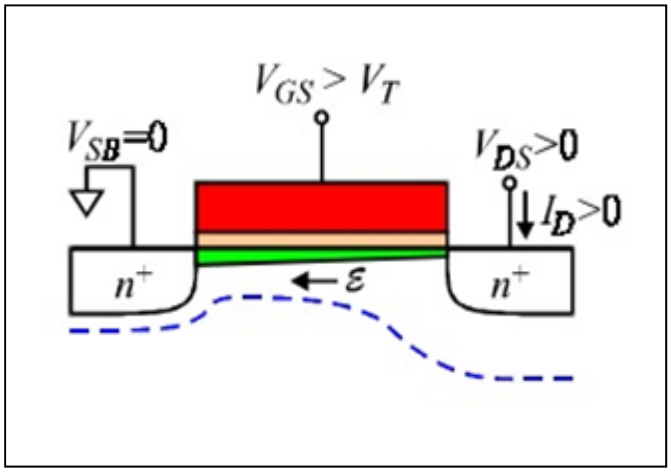

Fig 12: MOSFET in triode state [16]

current (Figure 12). As mentioned above, V_{DS} pushes the free electrons away from the drain electrode. If V_{DS} becomes too large, the electrons will be "pinched off" from the electrode and V_{DS} will cease to change the current across the device. Increasing V_{GS}, however, will still increase the current by increasing the density of free electrons [16]. See Figure 13 for an illustration of this state, known as saturation and Figure 14 for a graph of the triode and saturation regions of a typical MOSFET.

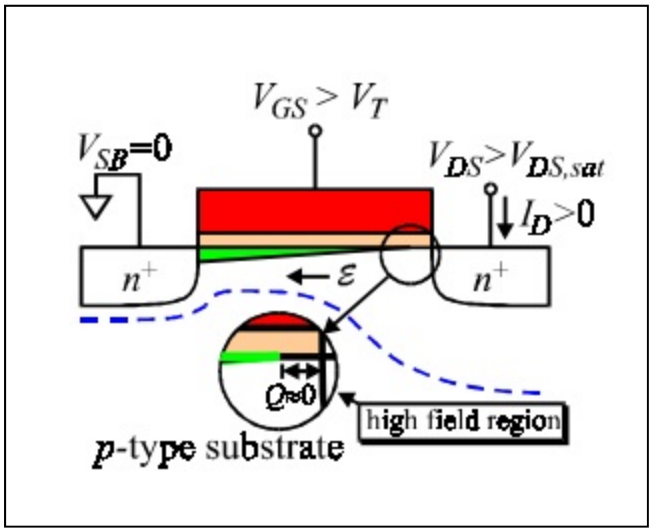

Fig 13: MOSFET in saturation mode [16]

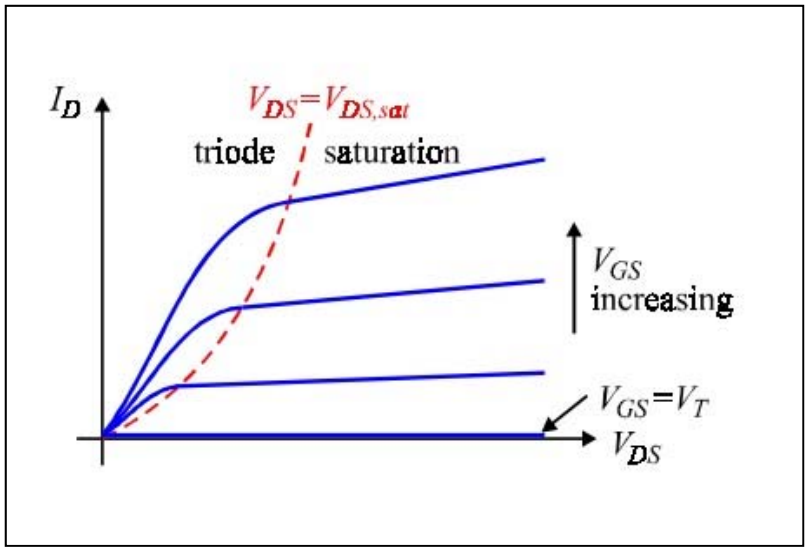

Fig 14: IV curve at various V_{GS} for MOSFET operation [16]

CHAPTER 2: OTHER METHODS TO FABRICATE GRAPHENE-BASED TRANSISTORS

There are currently several methods for producing transistors. The most common is photolithography, a process involving ultraviolet light and chemicals. Photolithography is easily able to fabricate silicon transistors, but when used with graphene, the devices are not always suitable for use. Research has been active in devising new methods for graphene transistor fabrication. Thermochemical nanolithography and thermal dip-pen nanolithography are two examples of such processes and are presented in this work.

2.1 Photolithography

Silicon transistors are currently manufactured by a process called photolithography, illustrated in Figure 15. This process can etch millions of devices simultaneously, and has

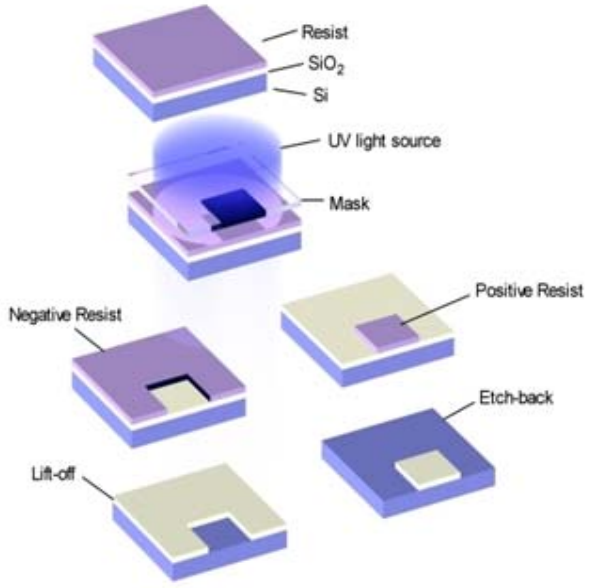

Fig 15: Illustration of the photolithography process [17]

been well established for decades. It is a method that can write shapes onto a silicon wafer by exposing the wafer to chemicals and light. Photolithography was employed to fabricate the samples used for this research and will thus be described in detail.

The first step is to clean the wafer of any defects such as dust, oil, or other impurities. Next, an insulating layer is deposited on the surface to act as a barrier to electronic conduction. This is usually silicon dioxide, which may be formed with high precision on the silicon substrate. The next step is to apply photoresist via centrifuge in a process known as spin coating. Photoresist is a chemical that will protect some areas of the wafer from etching. Spin coating deposits the photoresist evenly, which is important because the photoresist will later be etched away, and if it is not uniform, it will not etch correctly.

The photoresist comes in two varieties, positive and negative. For the positive one, the resist that is exposed to ultraviolet radiation will be chemically changed so that it is easier to etch. In short, “whatever shows, goes.” Thus, the mask is an exact pattern of the geometry of what is to be transferred to the wafer. Negative photoresists are more solidified by exposure to ultraviolet radiation. Therefore, wherever the resist is exposed is where the pattern will remain, so the mask is a “negative” of the pattern to be transferred. Positive resists are more popular because they offer better control for the fabrication of smaller features.

After the application of photoresist, the wafer complex is soft-baked. Baking makes the photoresist susceptible to light by removing most of the solvents from the resist. Baking too much will ruin the photosensitivity by either reducing its sensitivity to the developer or by destroying some of the sensitizer. Not baking enough will restrict the light from exposing the sensitizer. If a large portion of solvents remain in a positive resist, the resist will not be evenly

exposed. If the undersoft-baked wafer complex is developed, it will be less resistant to the etchant in both the exposed and unexposed areas, resulting in uneven etching.

The next step in the photolithography process is aligning the mask to the wafer. If there are multiple masks in the specific recipe, each one must be aligned to the previous pattern. The mask itself is a glass square with the desired geometry printed in chrome on one side. During the exposure phase, the printed geometry on the mask leaves a shadow on the photoresist protecting it from the ultraviolet light. The areas where light strikes are chemically modified so that they become easier to etch during the development stage.

During development, the photoresist is removed from the wafer so that the original substrate is revealed. Depending on the type of resist and the energy used during exposure, more or less of the photoresist will be present after development. Figure 16 shows curves representing the percentage of resist left after development as a function of the exposure energy. Variables such as thickness of resist, prebake conditions, the developer used and the time it is used, among other variables all affect the final outcome of the photolithography process. The number and complexity of these variables make finding the proper "recipe" time consuming and challenging.

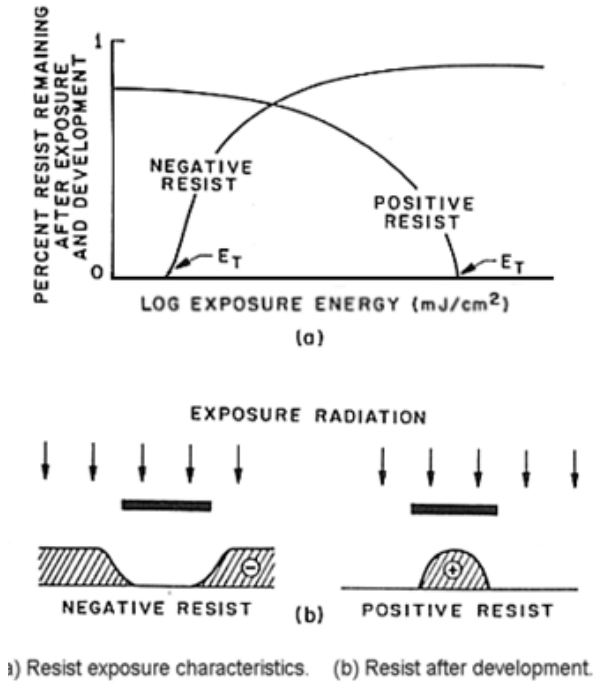

Fig 16: Effect of exposure on photoresist [18]

With the original substrate uncovered, it can now be etched to further shape the surface. Depending on the complexity of the geometry needing to be transferred, there can be multiple steps of etching, depositing photoresist or other materials, and exposing [18].

The entire process requires multiple steps that are very complex and depend greatly on every possible variable. Furthermore, the required chemicals can be very dangerous and are damaging to the environment. Similar processes can be used to shape graphene, but the edges of the "chicken wire" that remain are considered rough, and the edge effects negatively impact the electrical properties.

2.2 Thermochemical Nanolithography of Graphene Oxide

The Naval Research Laboratory has previously performed initial studies in using an atomic force microscope to fabricate a graphene transistor thin enough to be semiconducting but not suffer from rough edges. This work, published in *Science* in 2010 [6], was done on epitaxially grown graphene that was subsequently oxidized (Figure 17) and on isolated flakes of graphene oxide (Figure 7).

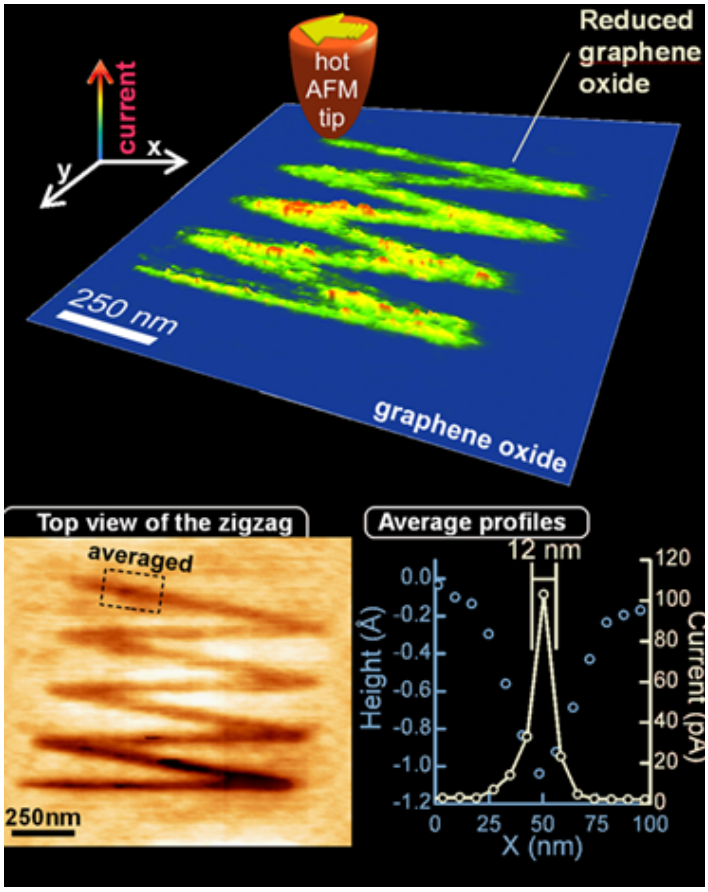

Fig 17: Illustration of the TCNL process [6]

The epitaxial graphene was fabricated by growing graphitic layers on hexagonal silicon carbide crystals. The process was done at 1300 ˚C in an ultra-high vacuum. Epitaxial growth is slow but not self-limiting, which means that many layers can be deposited, as many as 100 layers. After growth, one can determine the thickness of graphene using an Auger microscope. The graphene before oxidation had a mobility of 1100 cm^2 v^{-1} s^{-1} and structures can be deposited on the scale of an entire wafer [19].

The main results are summarized by Figure 17. As shown, the hot AFM tip moves over the graphene oxide, heating it to release the oxygen, thereby reducing it back to conductive graphene. The inset graph shows a height cross section of the device as well as the current carrying ability of the nanoribbon.

The thickness of this graphene used in Ref. 6 was not necessarily a single layer. Nevertheless, this research was successful in using thermochemical nanolithography to locally reduce a functionalized graphene surface back to the conductive form. It served as the motivation for this Trident project, in that we wished to expand the technique to new chemically-modified graphene of large-area and single layered.

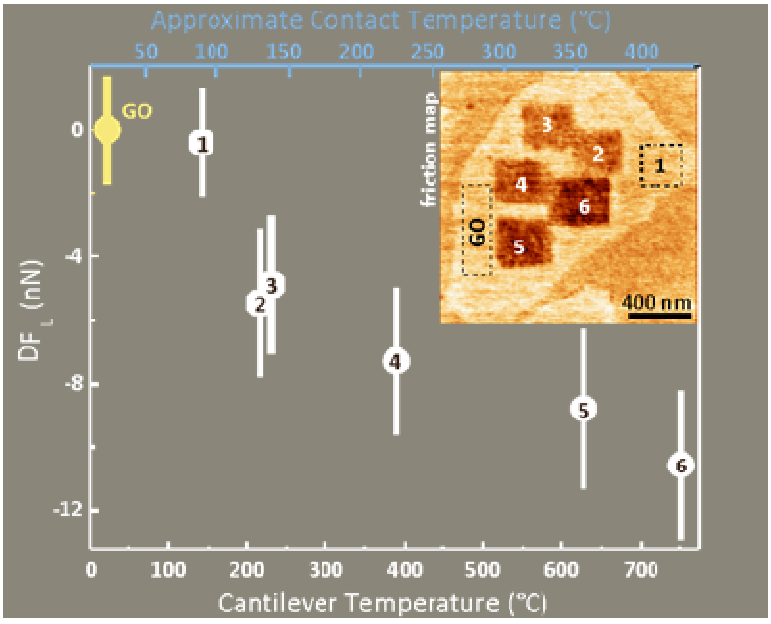

Fig 18: Effect of temperature on reduction of graphene oxide [6]

The graphene nanoribbons fabricated on the epitaxial GO were 12-100 nm thick and had a sheet resistance of 65 kΩ.

Furthermore, it was shown that the tip temperature affected the amount of reduction (Figure 18). By adjusting the current through the tip, and thus its temperature, squares were written at different temperatures ranging from 100-700˚C. The AFM friction image showed that the coefficients of friction changed continuously as the temperature increased [6]. This behavior is consistent with increased reduction as the amount of functionalized groups on the graphene decreased.

The surface of graphene oxide is actually composed of several different groups, not just oxygen. For example, there could be hydroxyl, carbonyl, as well as epoxy groups on the surface as well. Each group will require a different energy to liberate from the graphene, which is why as the temperature increased, more and more functional groups were reduced [20].

2.3 Thermal Dip-Pen Nanolithography

Another method of fabricating graphene transistors studied at Naval Research Laboratory is called thermal dip-pen nanolithography (tDPN). TDPN is a method of chemically isolating graphene nanoribbons, so that the high quality graphene can be protected while the remainder of the graphene is chemically modified to become insulating. It was studied in parallel with thermochemical nanolithography so that both methods can be compared to each other.

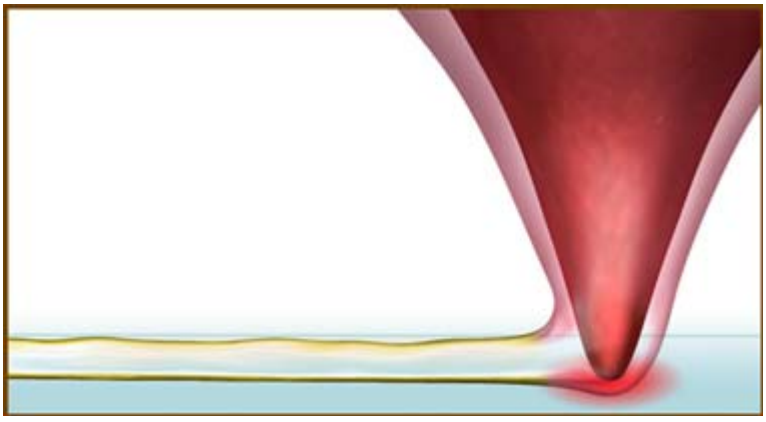

Fig 19: Polymer deposit onto surface from heated tip [5]

This process is accomplished by dipping an AFM tip in polystyrene and

heating the tip so that the polystyrene melts. The hot tip is then translated over a graphene surface fabricated via chemical vapor deposition [21]. The polymer is deposited on the graphene (Figure 19) and the polymer hardens as it cools. The entire sample is then exposed to XeF_2 gas to render insulating all the surface not masked by the polymer line. That is, since the polymer protects a thin line of graphene, that line does not get fluorinated. This allows a current to pass only along the thin underlying graphene ribbon that was protected. TDPN is summarized in Figure 20.

Polystyrene was chosen due to its hydrophobicity, insulating nature, and melting point. Lines as small as 35 nm with sheet resistances of 4500 Ω were produced using this method. It was found that faster writing speeds produced thinner devices. Also, this method produces devices that have clearly defined edges, which help maintain the electrical properties. The edges are not rough because the graphene itself is still intact. Therefore, the fluorine can be reduced off the graphene and the device can be reset if the polystyrene is dissolved away [22].

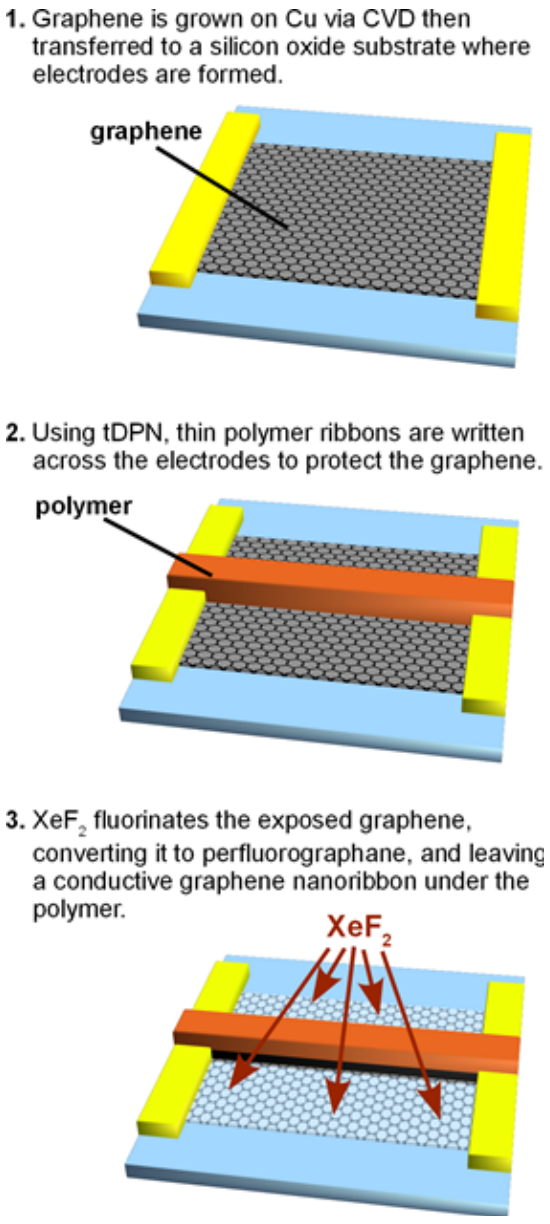

Fig 20: Illustration of thermal dip-pen nanolithography [5]

CHAPTER 3: EXPERIMENT-TCNL OF FLUOROGRAPHENE

This Trident project focused primarily on thermochemical nanolithography of fluorographene. The experiment was a proof-of-concept to determine if TCNL of single layer graphene was feasible. This chapter will explain the setup in detail. Also, a step by step guide of the process is included in Appendix A. The last part of this chapter will present some of the challenges encountered throughout the research.

3.1 Sample Fabrication

The fabrication of base-devices starts with the chemical vapor deposition (CVD) growth of graphene on a copper substrate [21]. The graphene is grown at temperatures up to 1000 ˚C in a methane and hydrogen atmosphere. CVD can grow large area films (~cm^2) of single layer graphene. Areas where the graphene was 2 or 3 layers thick can exist, but using the proper processing conditions and the self-limiting behavior of the process due to the low solubility of carbon into copper, this kind of growth is inhibited, and therefore more than 95% of the sheet is single layer. There have been claims that graphene produced in this manner can have mobilities up to 4050 $cm^2\ V^{-1}\ s^{-1}$. The initial mobilities for this project were on the order of 1500 $cm^2V^{-1}s^{-1}$.

After growth, a thin layer of polymethlmethacrylate (PMMA) is spun onto the graphene. Then, the copper is etched away and the PMMA/graphene is transferred from the etchant onto a 100 nm SiO_2/Si wafer where solvents remove the PMMA [22]. The graphene is afterwards shaped in rectangles via photolithography (the same process currently used to fabricate

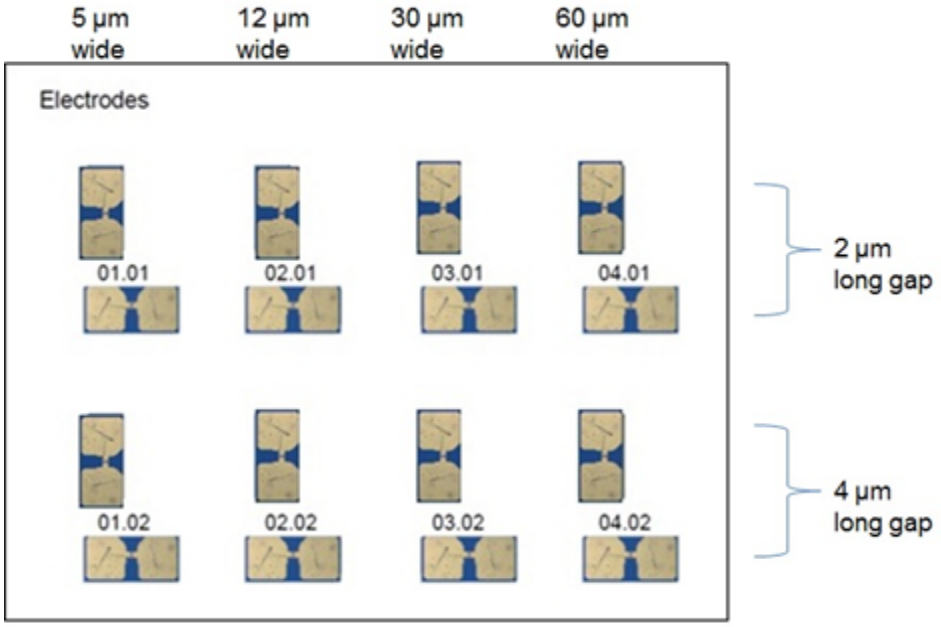

Fig 21: Electrodes arranged on sample

transistors) and oxygen plasma etching. 20 nm thick gold electrodes were formed via photolithography across the ends of each rectangle. These steps form the "base device," which has a length of either 2 µm or 4 µm and widths of 5 µm, 12 µm, 30 µm, or 60 µm, as shown in Figure 21. The devices were pre-screened for continuity. Devices with high resistance or open circuit were deemed unsuitable for further processing and discarded. Typical resistances of valid devices fell between 100 Ω for the largest devices and 2000 Ω for the smallest devices.

3.2 Functionalization: Forming Fluorographene

To render the graphene layer insulating, it must be fluorinated to fluorographene (C_4F). The fluorination process preserved the chicken wire lattice, but attaching fluorine to every fourth carbon opens the band gap to 2.93 eV. The fluorination is achieved by exposing it to XeF_2 gas via a Xactix XeF_2 etcher. Typically 12 to 15 cycles of 1 minute exposure were sufficient to render the devices fully insulating. After each exposure cycle, the atmosphere was purged so that fresh gas was introduced for the next cycle.

In most cases, the smaller devices (5 and 12 µm wide) consistently became fully insulating, carrying an electric current less than 10^{-13} A to 10^{-15} A, with no voltage dependence. Figure 22 shows the current-voltage characterization for a typical open device. The current is on the order of 10^{-13} A and is primarily due to a small leakage current.

The typical effect of the fluorination on the resistance of the largest (30 and 60 µm wide) devices was an increase of several orders of magnitude. The devices are, however, rarely fully

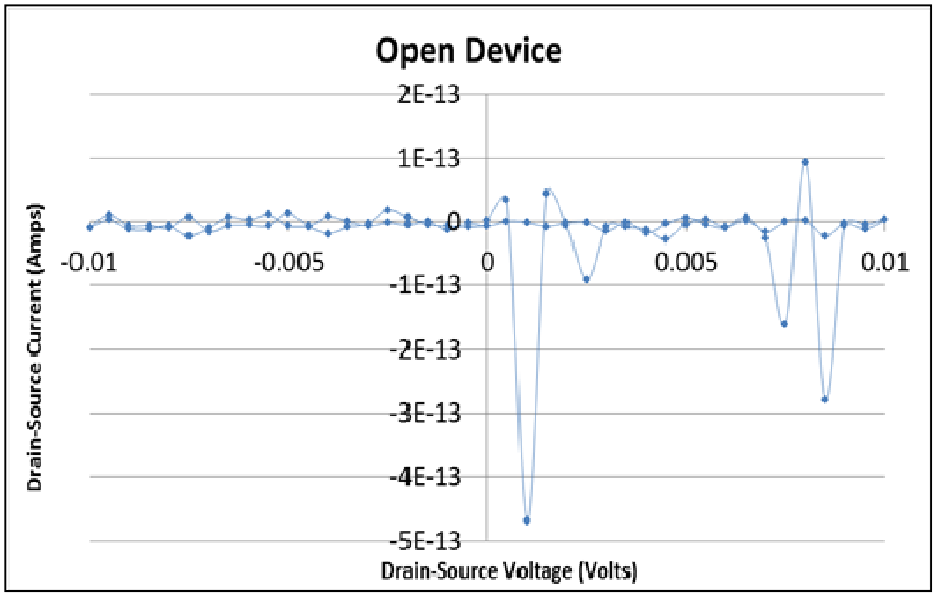

Fig 22: IV curve for an open circuit device

open circuit. Consequently, for the purpose of this study, we avoided using these large devices and concentrated on the smaller, open circuit devices.

3.3 Reduction

After the samples are prepared and the baseline measurements complete, the devices are ready to be locally reduced back to conductive graphene by thermochemical nanolithography. A step-by-step process can be found in Appendix A. In general, an atomic force microscope (Asylum Research, CA) is used to image the device before reduction so that the lithography pattern can be defined. When ready to fabricate, a current of 5.5 mA (25.6 mW of power) was applied to the tip and a line drawn using 1 V of deflection setpoint (the force the tip exerts on the surface) at a speed of 20 nm/s. The heater temperature is approximately 700 °C; however, the temperature at the contact between the probe and the fluorographene would be significantly less, about 400 °C. All motions are controlled by the AFM's associated MicroAngelo^{TM} lithography software. We use 5.5 mA heating current, as it is the largest current output the tip can handle before turning red with heat. The writing process takes only a few minutes, after which the

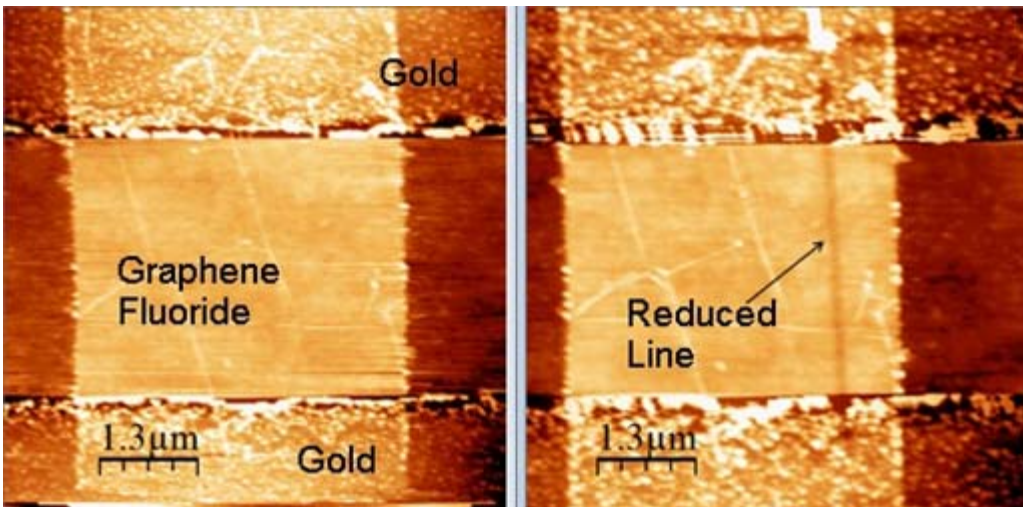

Fig 23: Graphene samples before (left) and after (right) reduction

current is turned off and the device is reimaged to visually inspect what changes, if any, are observable. Figure 23 shows the AFM height images of both before and after reduction. The written line is clearly visible in the “after” image.

3.4 Challenges

There are several challenges that arise when performing the reduction process. Hysteresis, controlling the tip’s position, the quality of the original graphene, and controlling the temperature of the tip are major examples. Other complications include keeping the tip sharp, finding the proper reduction atmosphere, and fabricating tip holders that enable current to flow through the tips.

A major issue with all atomic force microscopes is hysteresis. When the tip scans over the surface, it doesn’t move. In fact, the sample is what scans back and forth. The AFM uses piezoelectric translators to actuate this motion, and they sometimes shift slightly. Thus, from one scan to another, the image can migrate several nanometers. This migration is called hysteresis. The issue with hysteresis is that the AFM needs to image the surface first so that the pattern can be defined. Thus, if hysteresis affects the next image, the line could be drawn a few nanometers off of where it was supposed to be. As long as hysteresis affects every line the same magnitude and direction, this shouldn’t be a major problem. Also, in an industrial environment, perhaps the AFM won’t need to pre-image the devices. However, the best way to reduce this problem would be to use the best atomic force microscope possible.

A similar problem to hysteresis is controlling the location of the AFM tip. While hysteresis only affects the lateral position of the tip, a critical issue is the load on the probe. Specifically, if the tip does not contact the surface, the heat will not reduce the fluorographene.

However, if the tip pushes too hard, it could break the graphene. These two problems may be overcome by adjusting the deflection setpoint (i.e., the load on the tip).

A third challenge stems from the presence of the 20 nm thick gold electrodes deposited on top of the graphene. Therefore, there is a change in height of 20 nm between the gold and the graphene. Because the tip has a finite sharpness, when it writes the line going from the gold to the graphene, it can skip a small part of the graphene touching the electrode, as described by Figure 24, leaving a gap between the transistor and the electrode from which measurements are made. This reduces the accuracy of the electrical measurements.

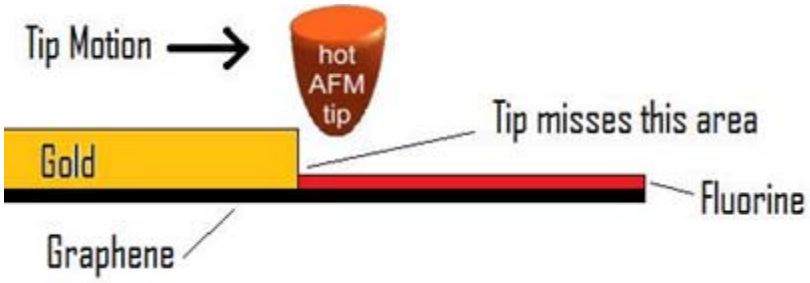

Fig 24: Tip skipping off of gold electrode

To overcome this problem, the tip was moved at slower speeds when making the transition from gold to graphene. This allowed the tip more time to be in contact with the surface. However, when writing an integrated circuit on a fluorographene surface, this problem will be non-existent because there will be no gold electrodes to interrupt the tip contact.

Perhaps the greatest challenge is the quality of the original graphene. Because CVD graphene was only discovered 24 months before the start of this research, the means of growing and transferring it continue to evolve to this day. The starting material can sometimes have a low mobility, and the fabrication process can leave residue and impurities on the surface. It is important for the graphene to have an initially high mobility so that it will have a high mobility

after TCNL. Also, the impurities can interfere with the fluorination and reduction process. There is currently much research being done to fabricate large areas of high quality and to do so quickly and cheaply. Some researchers claim to have produced CVD graphene with mobilities of 100,000 $cm^2 V^{-1} s^{-1}$ [23].

Other issues, such as temperature control and tip sharpness can be more easily overcome. Using a controlled system to apply current and measure the temperature has already been implemented into the atomic force microscope, and diamond coated tips will help maintain tip sharpness. A carbon nanotube tip will also enable smaller devices and more precise fabrication. Performing the reduction in air is problematic as the humidity negatively affects the reduction. Consequently, most of this research was done in a nitrogen atmosphere but forming gas, a mixture of 10% hydrogen in argon, has been known to enhance the speed of reduction. See section 5.3 for data analysis.

The last major problem encountered during this project was converting the AFM tip holders to work within the parameters of the project. The AFM has a "tip holder" that detaches from the microscope to facilitate changing the tip. Most holders are not designed to flow a current through the tip, so a specialized device had to be made to flow a current through the

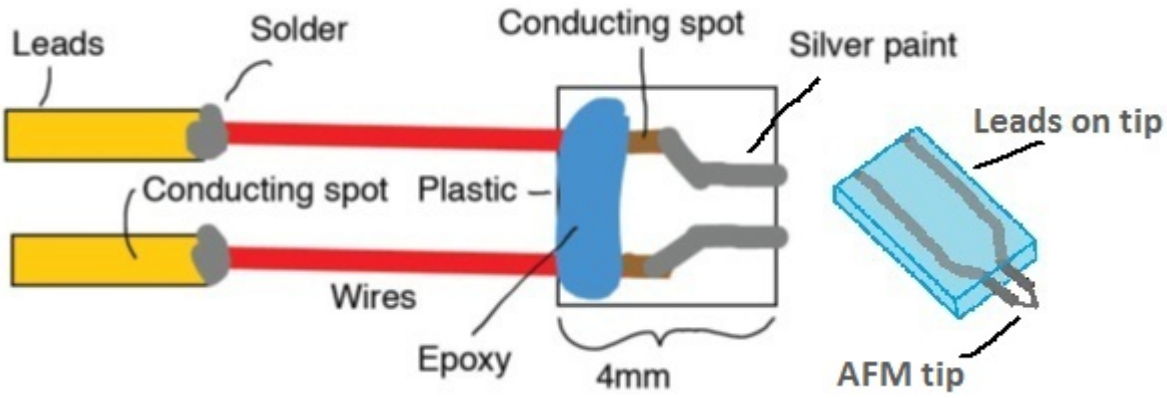

Fig 25: Tip holder adapter designed by author and AFM tip

specially designed tip and prevent a short across the leads. Figure 25 shows the adapter that the author designed and made. It uses a plastic square to prevent shorts, and silver paint connects to the leads on the tip to the wires. The wires are secured by epoxy and soldered to leads so that the current will flow through the cantilever and heat the tip.

CHAPTER 4: CHARACTERIZATION

To determine if thermochemical nanolithography was successful, the electronic properties of both the initial and final devices must be measured. This chapter will present the data on the physical analysis of the devices taken immediately after TCNL is complete. It will also show that electrical characterization is needed to truly determine the results of TCNL.

4.1 Physical Characterization

Figure 23 shows that there is clearly an effect of the tip passing over the fluorographene layer. Using this AFM height image, a cross section can be made to determine the full width of

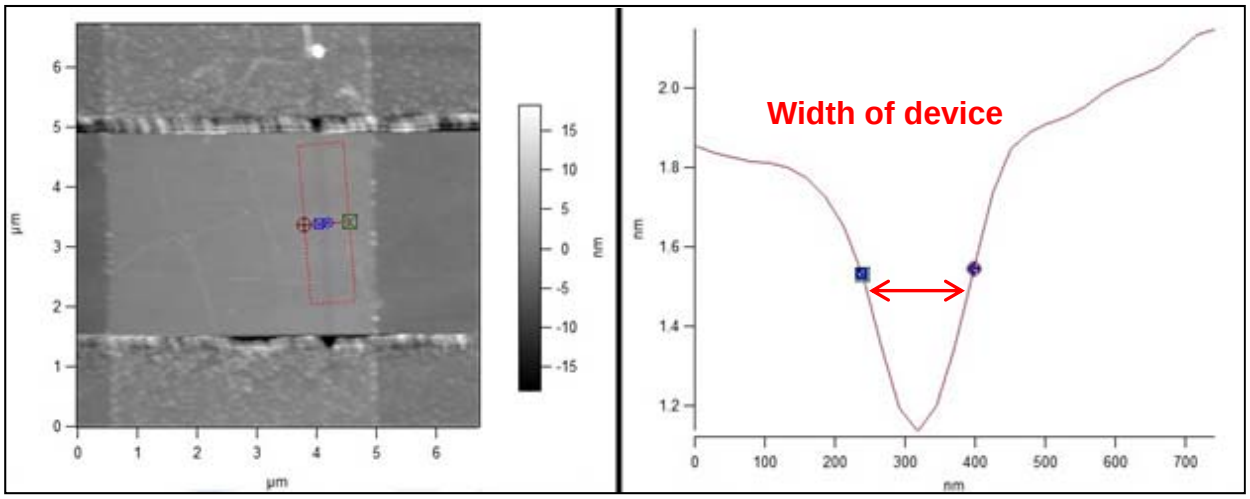

Fig 26: Section image across device in Figure 23

half maximum (FWHM) of the reduced line, shown in Figure 26.

The image below shows a line that is 120 nm wide and 650 pm deep. The image on the left shows that the section was averaged over the red rectangular box and the line itself is barely visible. In the height image, a barely visible line is a good indication that the reduction process worked, since we only expect a change in height of a few angstroms. To see the line more clearly, the friction image is used; see Figure 27. Unfortunately, the friction data is also more susceptible to noise, as evidenced by the alternating horizontal dark and white bands. Since the friction data is collected from the lateral twisting of the tip, the AFM is sensitive to small vibrations that get picked up as noise. The

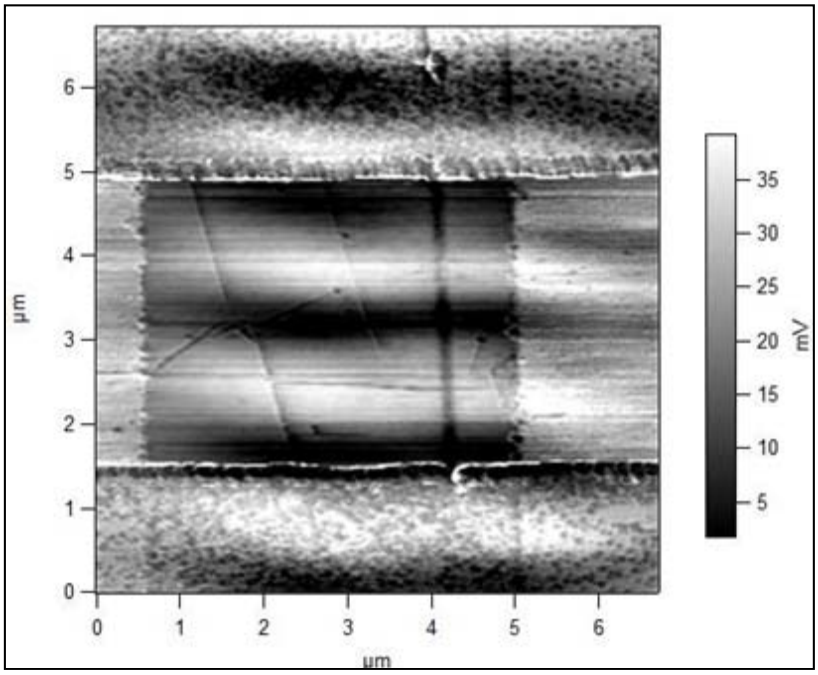

Fig 27: Friction image of device in Figure 23

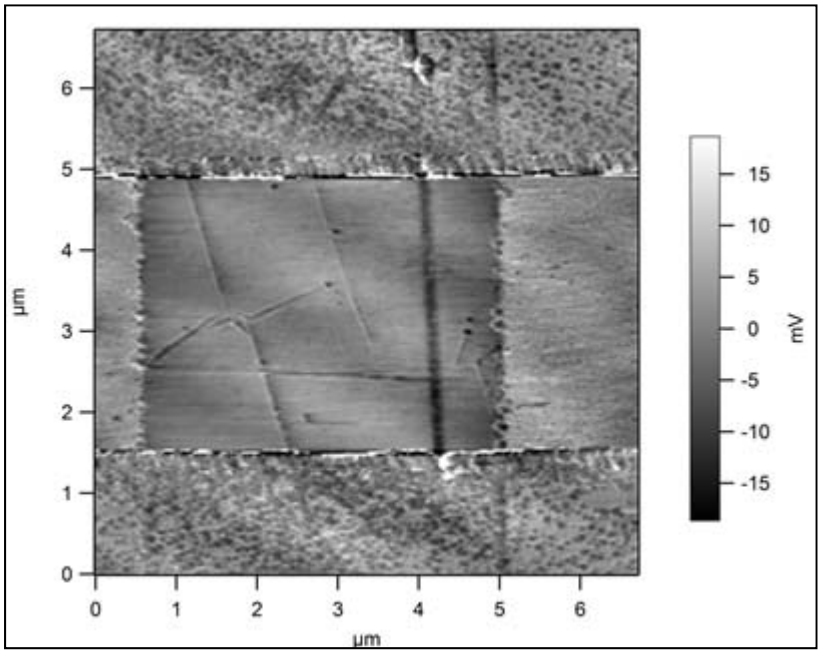

Fig 28: Friction image after flattening

noise can be cleaned up by performing a “flatten” function on the AFM software, the effects of which are shown in Figure 28. Flattening works by fitting each new row of data with a line which is then subtracted from the data. This reduces row to row variations in height.

Figure 29 shows another view of this same device. Since the atomic force microscope records the topography information in three dimensions, the height image can also be displayed in different perspectives. This image allows one to see the reduced line more clearly, and another cross section was taken along the blue line. The section data is graphed in Figure 30.

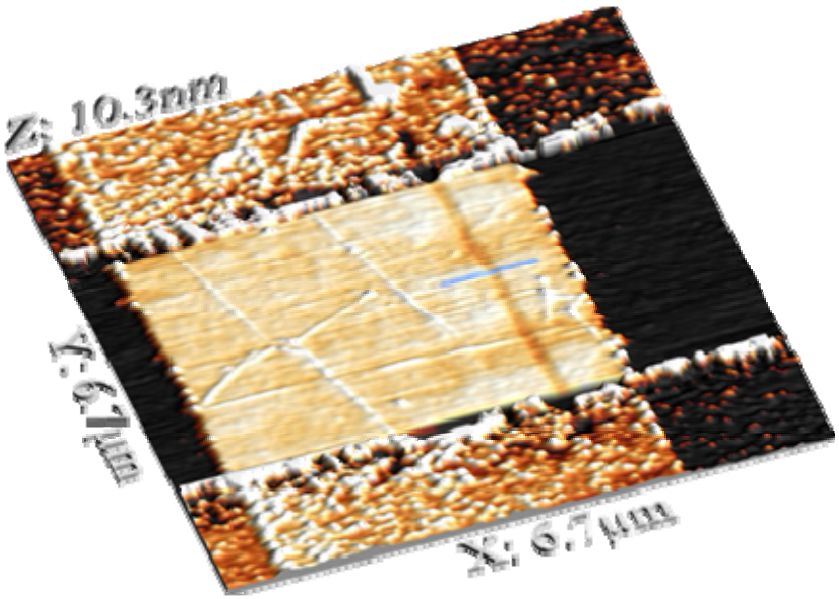

Fig 29: 3D height image of rFG nanoribbon

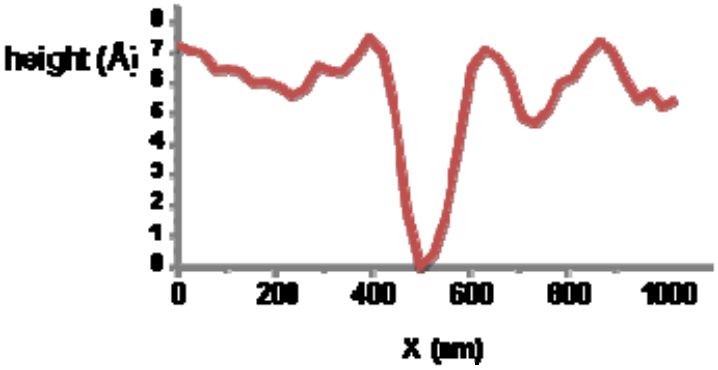

Fig 30: Section across rFG nanoribbon

Devices that are 100 nm wide are reproducible and there is potential for narrowing the devices further. We currently use a silicon heated probe for this experiment, which dulls as it is used. As mentioned previously, a diamond coated tip, or a carbon nanotube tip will eliminate this issue.

Depths on the order from 200-650 pm were observed. The actual depth, however, is difficult to determine due to the fact that impurities on the surface of the graphene are also read by the AFM cross section. Nevertheless, these depths are reasonably due to reduction because of the length of a carbon-fluorine bond and the difference in topography of sp^2 and sp^3 graphene gives changes in height of similar orders of magnitude.

4.2 Electrical Characterization

Unfortunately, the question if the reduction was successful cannot be answered only through the height images. Indeed, the height difference could be due to the tip scraping away impurities on the surface of the fluorographene. To determine whether the fluorographene was truly reduced, electrical characterization is required. Figure 31 shows the electrodes across which the currents and voltages were measured.

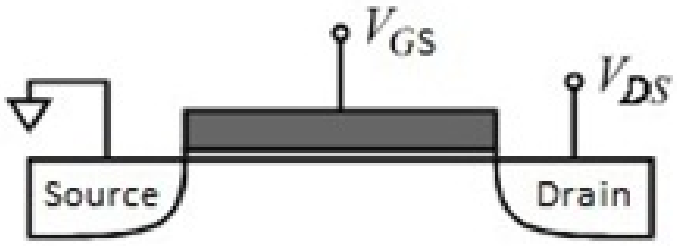

Fig 31: How measurements were made [16]

Figure 32 is an image of a probe station that is similar to the one used to make the electrical measurements in this Trident project. The sample is placed on the stage under the microscope and probes are brought into contact with the gold electrodes by the use of high turn density screw translators. In the case of Figure 33, the FG in the "before" image was completely insulating, defined as passing a current of 10^{-13}A. In the "after" image however, the device passes a current of nano-amps (~10,000x higher), and the resistance fell to 2 MΩ, as shown in the current-voltage graph in the "after" panel. Therefore, the initial electrical characterization shows that the reduction was successful and that the graphene device was successfully written.

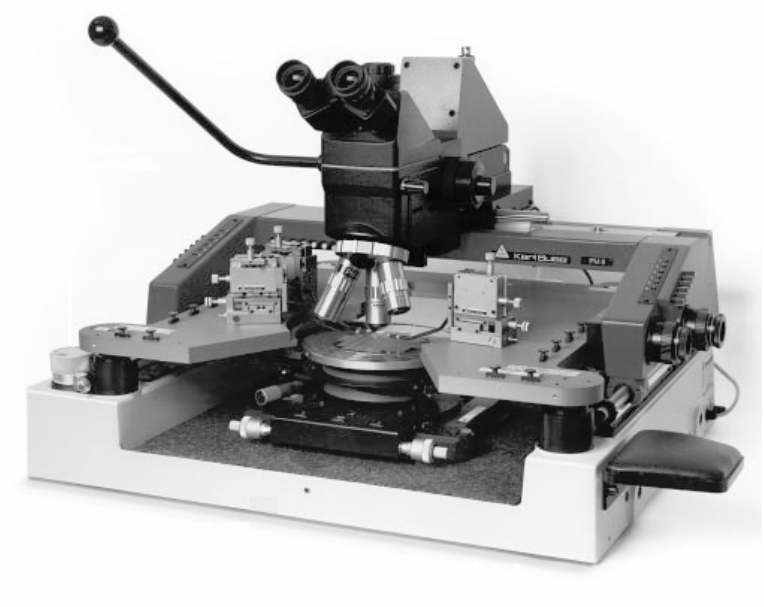

Fig 32: Probe station where measurements are made [24]

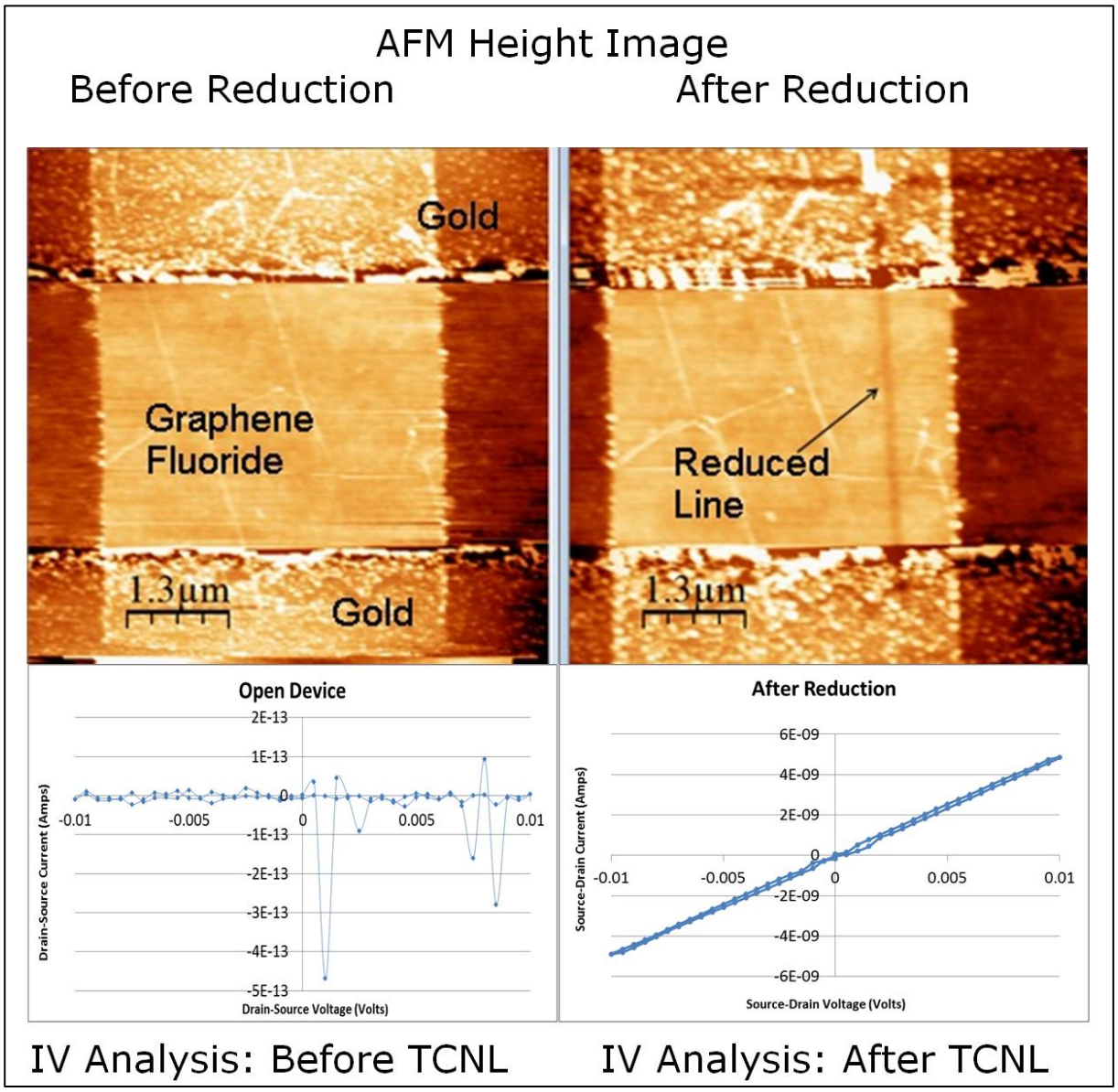

Fig 33: Electrical characterization of the device in Figure 23 before and after reduction

It is also important to evaluate the response of the nanoribbons to different gate biases. The doped silicon wafer is used as the back-gate. Figure 34 shows results for a typical device. Such results indicate that the device exhibits a field effect, which is necessary for transistor operation.

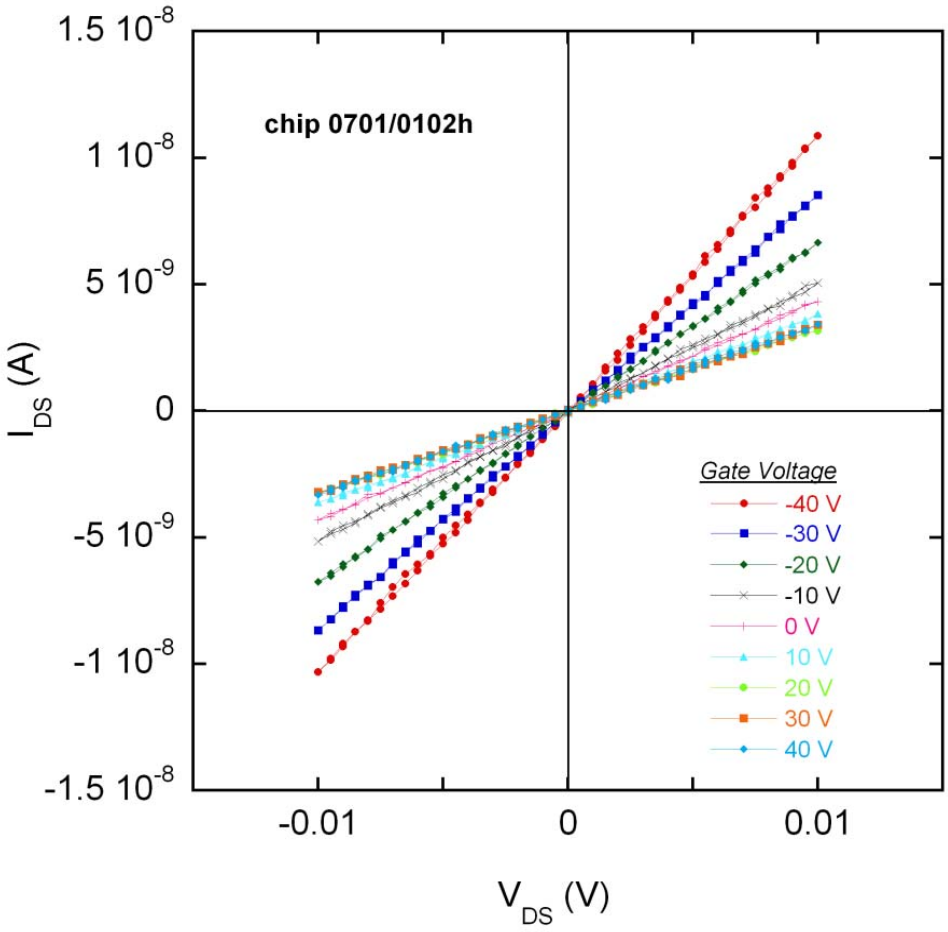

Fig 32: Observed field effect of Figure 23 device

A field effect means that one can control the current across the electrodes by applying an external electric field. This "gating" effect is what controls a transistor acting like a switch, either on or off.

The transconductance information from Figure 35 can be used to find the mobility of the reduced material. The transconductance is the change in the drain-source current for every volt applied to the gate. In other words, it is the slope, or derivative, of the curve shown in Figure 21.

Typical mobilities for the reduced devices are 18 or 20 cm^2 V^{-1} s^{-1}. These values are about 20 times higher than that of amorphous silicon [25] and 200 times higher than conductive

polymers [26]. Unfortunately, the initial graphene mobilities for this specific device were not determined, so it is impossible to precisely say how TCNL affects the mobility. However, other devices had initial mobilities on the order of 1500 $cm^2\ V^{-1}\ s^{-1}$, so it appears that TCNL reduces the mobility by two orders of magnitude. Equation (1) shows the formula used to calculate the mobility.

$$\mu_h = \frac{\Delta I_{DS}}{\Delta V_{GS}} \frac{L}{W V_{DS} C_g} \qquad (1)$$

where $\Delta I_{DS}/\Delta V_{GS}$ is the transconductance, L is the device length, W is the device width, V_{DS} is the potential across the source and drain, and the effective capacitance, C_g is $2x10^{-8}$ F cm^{-2}.

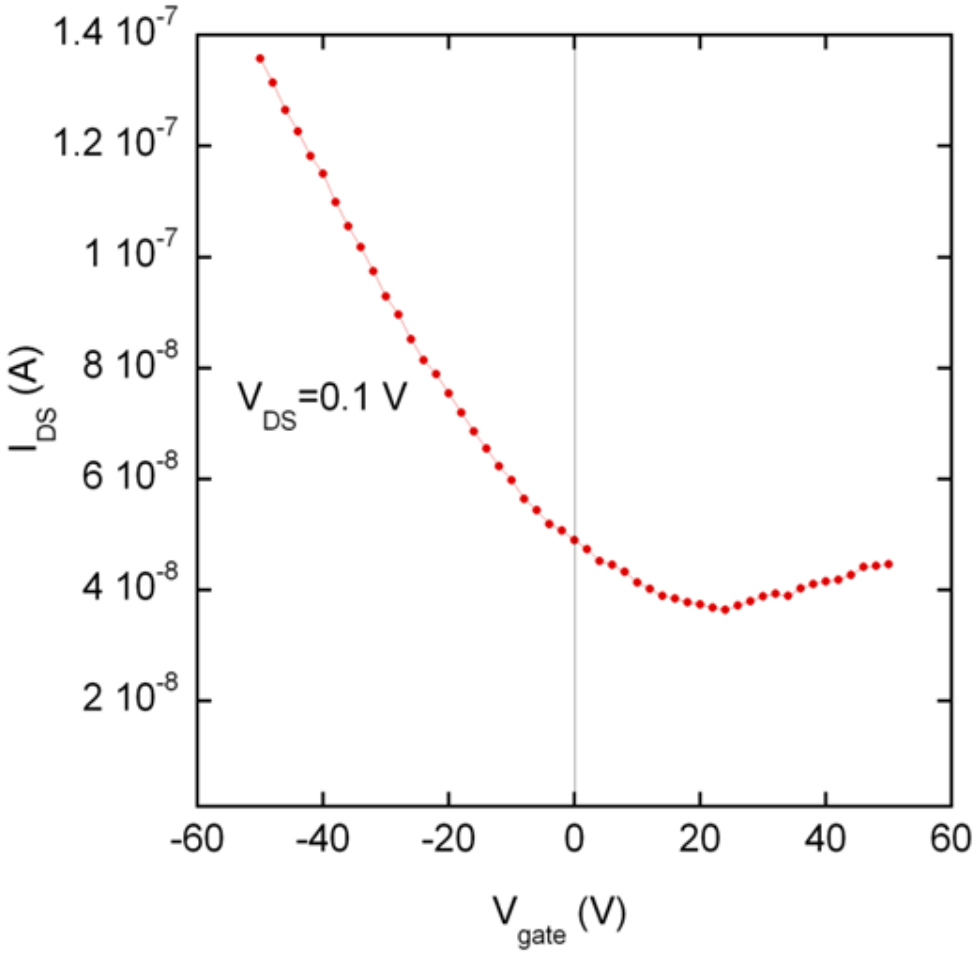

Fig 35: Transconductance measurement of Figure 23 device

4.3 Sheet Resistance

The resistance of devices will vary depending on the size of the device. Resistance is inversely proportional to width and directly proportional to length. This means that the longer the device, or the thinner the device, the higher the resistance. Therefore, to compare devices of different sizes, an intrinsic value must be measured. Sheet resistance (Eqn. 2) is the most appropriate quantity. It is calculated by multiplying the resistance by the width and then dividing length.

$$R_{sheet} = \text{Resistance x width x length}^{-1} = \rho / \text{thickness} \qquad (2)$$

Essentially, sheet resistance is thus the resistance per square. This is different than simply dividing the resistance by the area of the graphene ribbon as two ribbons can have the same area, but drastically different resistances. See Figure 36 for an illustration. Both graphene ribbons have

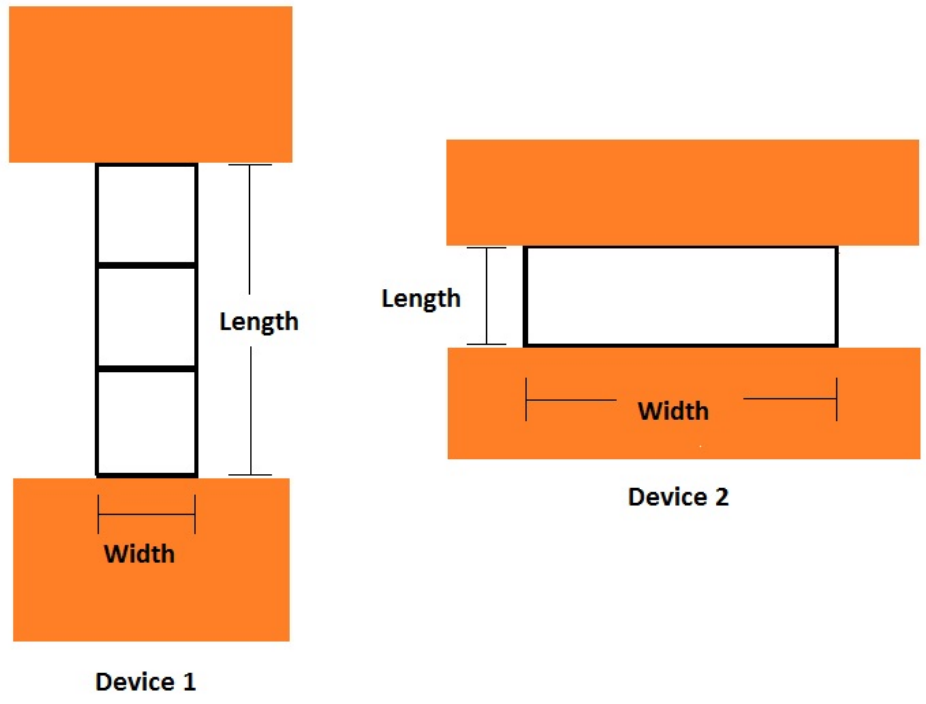

Fig 36: Explanation for importance of sheet resistance

identical areas, but Device 1 will have a larger resistance because it is longer and thinner. In equation 2, ρ represents the resistivity of the material, which is an intrinsic property to every material. Assuming that the thickness of the graphene is constant between the devices means that the sheet resistance, or resistivity divided by thickness, is an intrinsic property that allows comparison between devices.

The devices in this study typically had sheet resistances of 25 to 250 kΩ. This value will vary based on the quality of the initial graphene and the amount of reduction. If higher quality graphene is used to make the samples, the sheet resistance will be lower. Also, the more the fluorographene is reduced, the lower the sheet resistance will be.

CHAPTER 5: EFFECTS OF CHANGING REDUCTION VARIABLES

More information on the reduction mechanism during the thermochemical nanolithography process can be extracted from the study of the effect of changing process parameters on the properties of the final device. This chapter will discuss how the tip temperature and the writing speed affect the final device's width, amount of reduction, and the depth of the trench.

5.1 Changing the Tip Temperature

One of the tests performed was writing five lines each at different temperatures. The temperature was controlled by specially designed software implemented into the atomic force microscope controller. This software was developed in the King Group in the Department of Engineering at the University of Illinois at Urbana-Champaign. Each line was written at 20 nm/s with 1 V deflection setpoint. The temperature was increased for each line, and the temperatures used were 100 ˚C, 160 ˚C, 200 ˚C, 270 ˚C, and 330 ˚C. This control setup was unable to use higher temperatures because the controller was limited to 10 V. Figure 37 shows the experimental setup with line 1 being written with the lowest temperature and line 5 being written with the highest temperature.

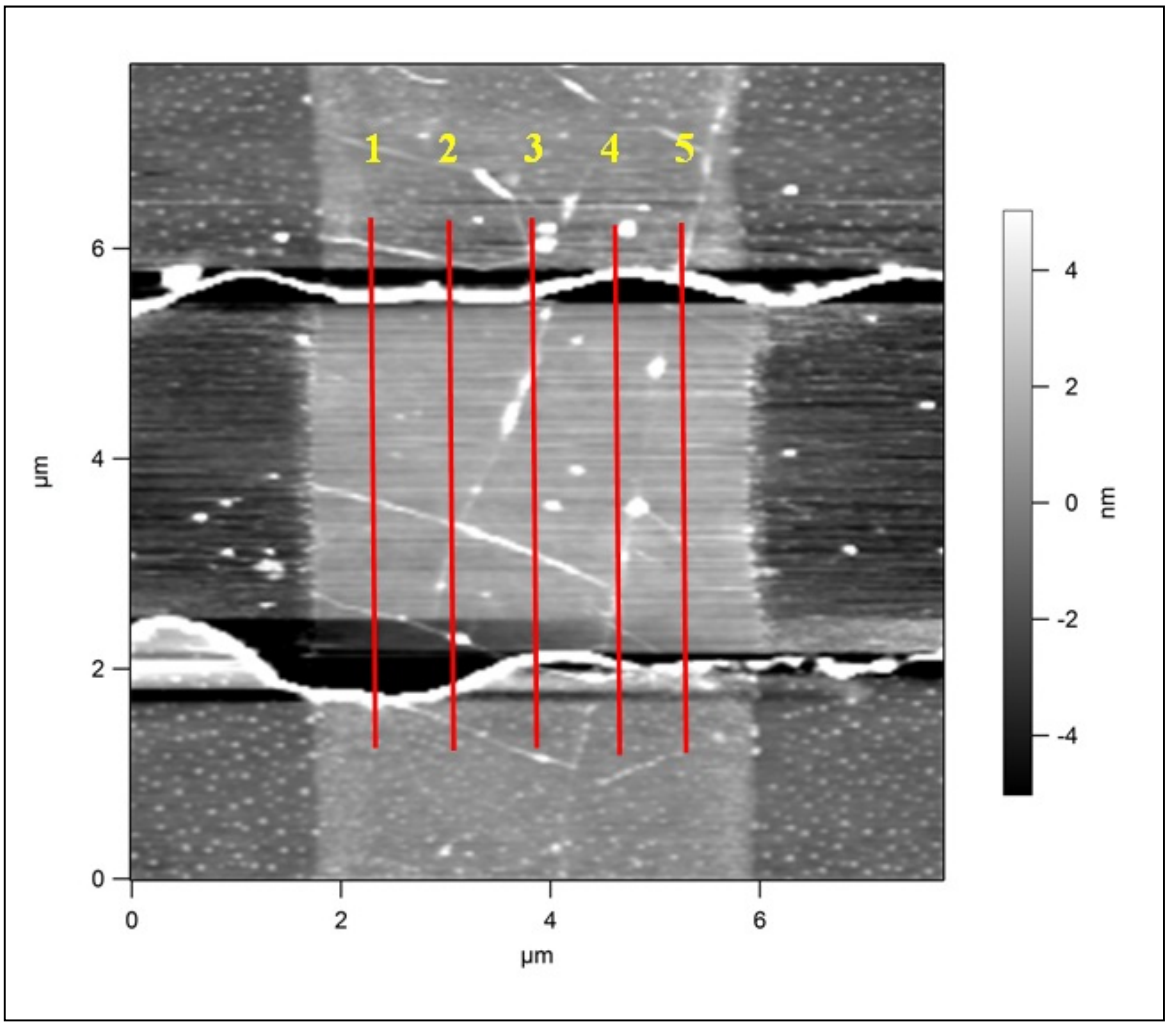

Fig 37: Variable temperature test

The expected result of this test would be that the higher temperature used to write the device would result in a higher amount of reduction, as there is more energy in the same amount of time to reduce more fluorine off of the graphene. After writing the lines and re-imaging the device, the results were found to be different from expectations. Figure 38 shows that only the highest temperature line was reduced.

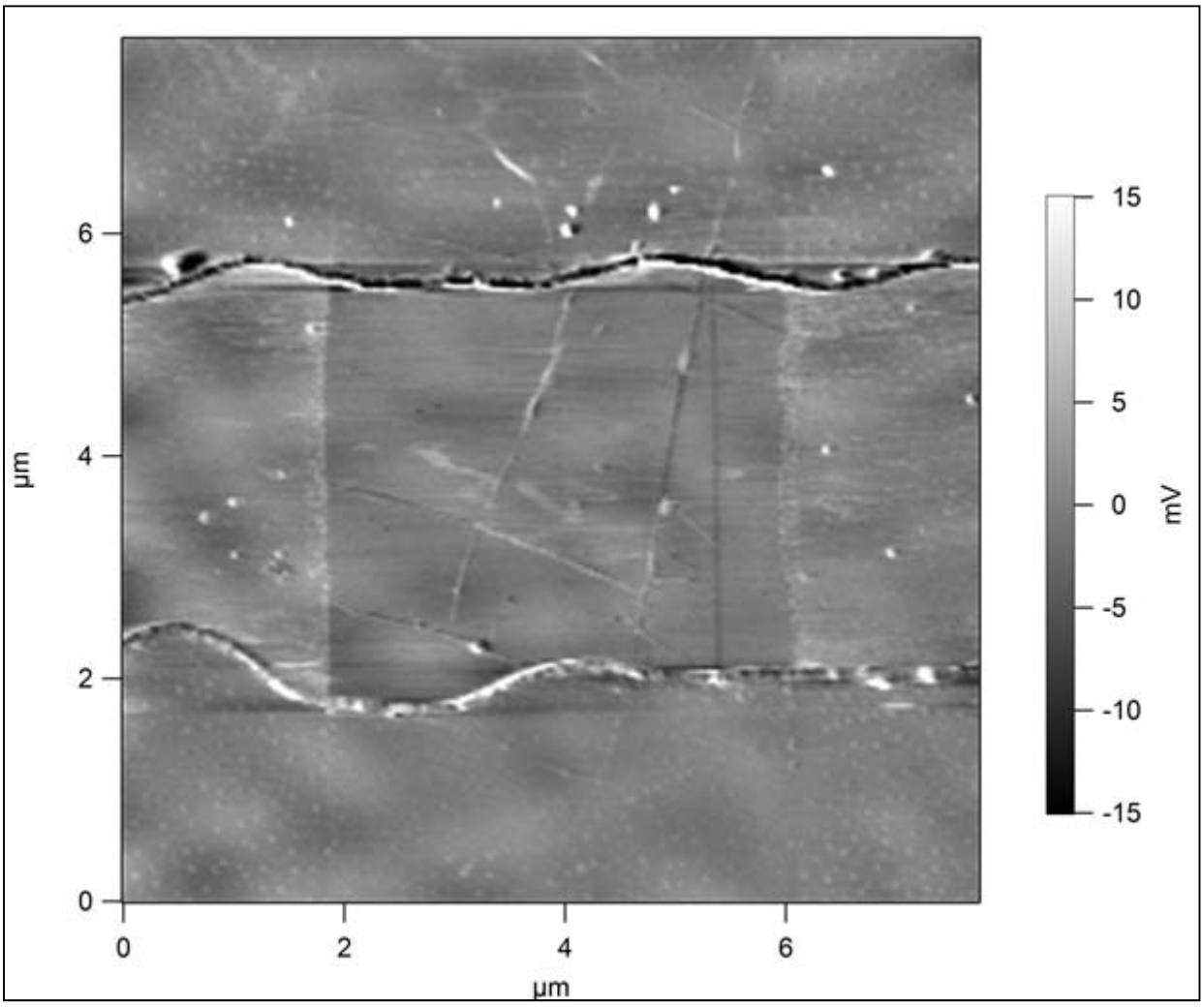

Fig 38: Results from the variable temperature test

These results are consistent with the fact that lower chemical diversity in fluorinated graphene would enable a crisper and more robust reduction. In contrast, recall the previously published research on graphene oxide where it was shown that the higher the tip temperature used to write on graphene oxide, the more functional groups were reduced away (Figure 18). Fluorographene, however, only has one functional group, fluorine. Therefore, assuming that the calibration data used to find the temperature of the tip is correct, the temperature needed to reduce fluorographene back to graphene is greater than or equal to about 300 ˚C.

Unfortunately, there are questions regarding the accuracy of the calibration data using the controlled setup. The controller is limited to ten volts, but the calibration scale assumes that the voltage is not limited, thus there may be an inconsistency between the actual temperature of the tip and the displayed one. Nevertheless, the sharp temperature onset of reduction points towards fewer functional groups in fluorographene compared to graphene oxide.

Due to only one line being successfully written at the highest controlled temperature, the effect of temperature on the device's width and depth could not be determined. Because the heat transport from the probe into the substrate is ballistic, meaning the heat doesn't "scatter" chaotically, one expects ribbon width comparable to the contact radius. However, there will be some heat diffusion near the contact so it is expected that higher temperatures should produce devices with slightly higher widths. It is also expected that the conductivity increases with more reduction. Thus, if higher temperatures than those available with the experimental setup are used, one should be able to experimentally confirm or deny these expectations.

5.2 Changing the Writing Speed

Another important variable whose effect on reduction needs to be understood is tip writing speed. By holding the temperature of the tip constant and writing lines at different speeds, one can study how the width and friction image change. The expectation for this experiment was that the faster the tip moves, the less time available for reduction, thus the less reduced the fluorographene will be. The experimental setup was almost identical to Figure 35, except that a different device was used. Line 1 was written at 20 nm/s, line 2 at 30 nm/s, line 3 at 40 nm/s, line 4 at 50 nm/s, and line 5 was written at 60 nm/s. All the devices were written at an approximate temperature of 700 ˚C.

Figure 39 and Figure 40 show the height and friction images, respectively, of this test. Figure 41 and Figure 42 are the sections across each line that show the width and change-in-friction data for the height and friction images.

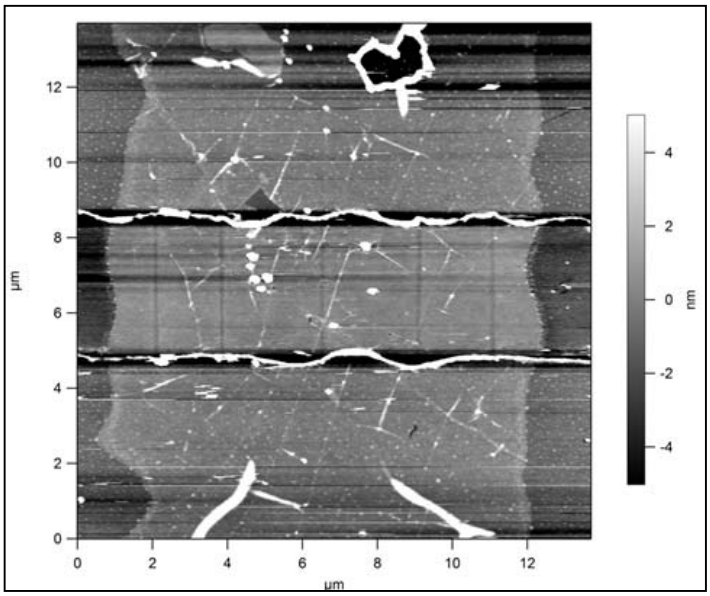

Fig 39: Height image from variable speed test

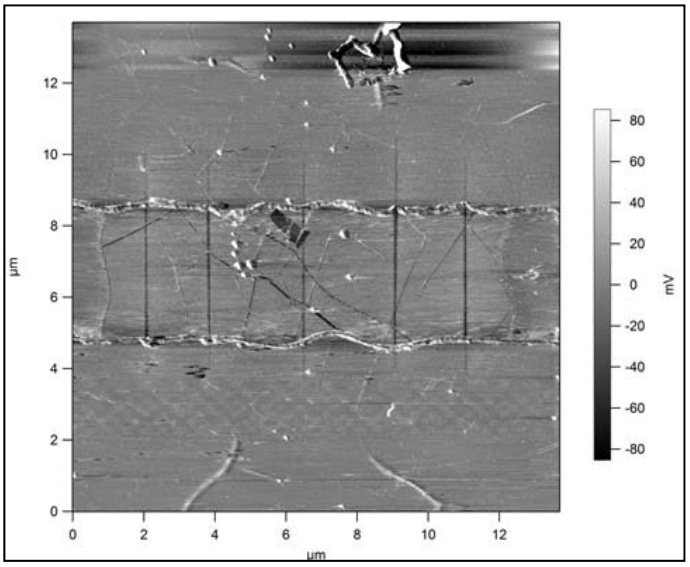

Fig 40: Friction image from variable speed test

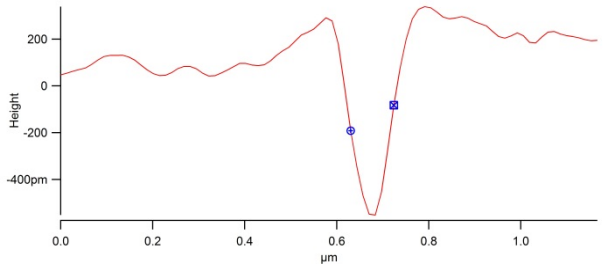

20 nm/s: 93 nm wide

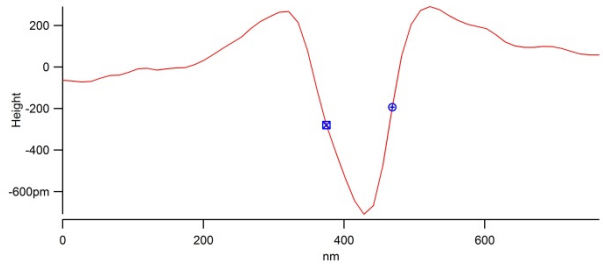

30 nm/s: 93 nm wide

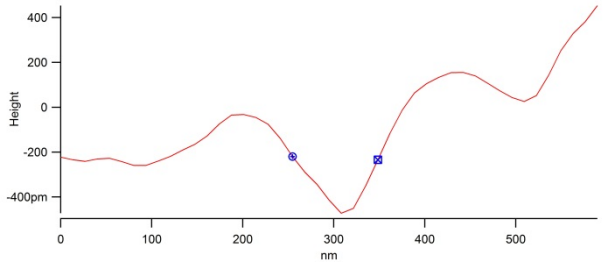

40 nm/s: 93 nm wide

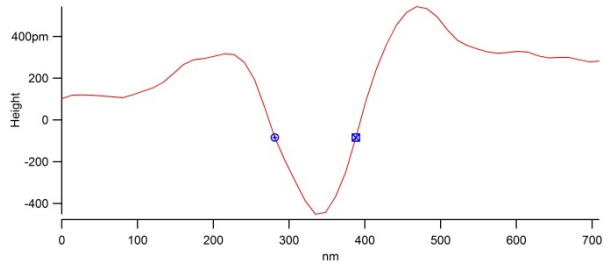

50 nm/s: 107 nm wide

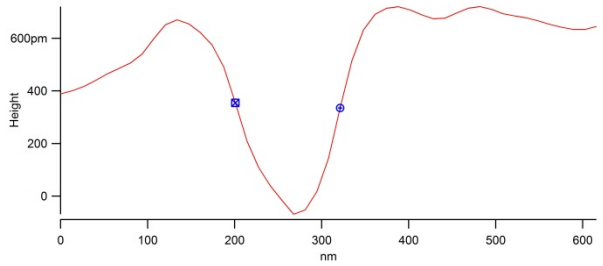

60 nm/s: 120 nm wide

Fig 41: Height section images for variable speed test

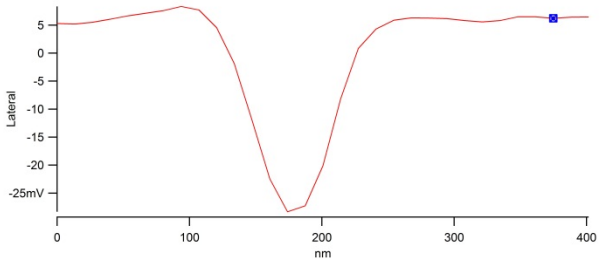

20 nm/s: 30 mV difference

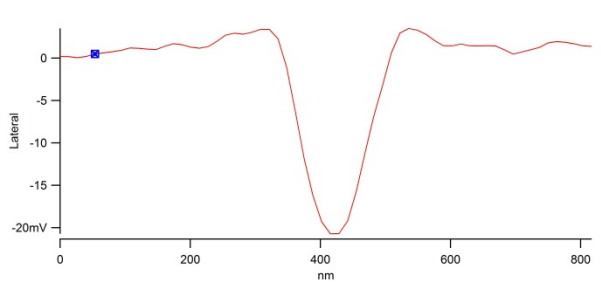

30 nm/s: 20 mV difference

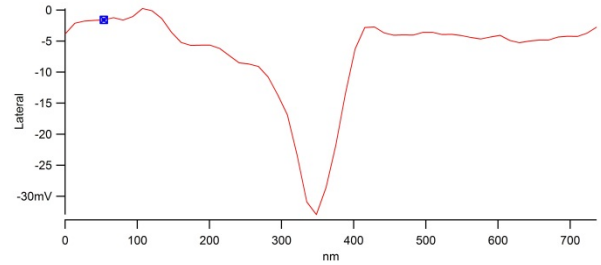

40 nm/s: 30 mV difference

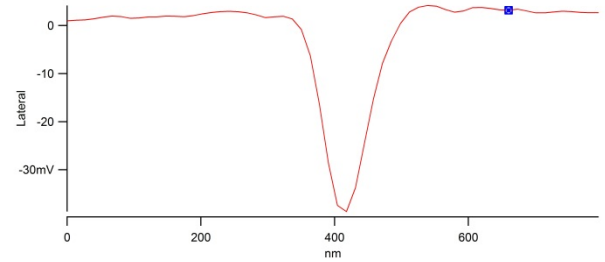

50 nm/s: 40 mV difference

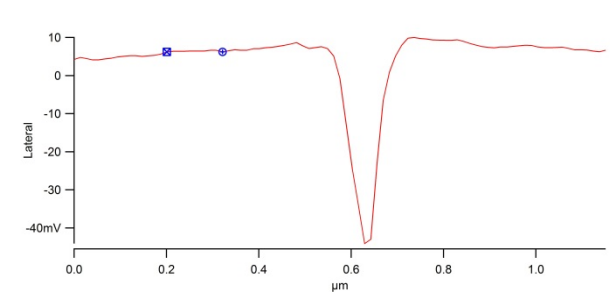

60 nm/s: 45 mV difference

Fig 42: Friction section images for variable speed test

From Figure 41, the expectation for the variable speed test was wrong. It was thought that the width would be inversely proportional to speed, but that is clearly not the case. Also, Figure 42 shows a similar disparity in the friction data.

5.3 Effect of Forming Gas

Forming gas, a mixture of 10% Hydrogen in Argon, is known to enhance the reduction process. TCNL was also performed in this atmosphere and was shown to have promising results. Figure 43 shows two devices written in forming gas, and they have better properties than devices written in N_2. The device is 40 nm wide, 500 pm deep, and was written at 10 nm/s at 600 ˚C.

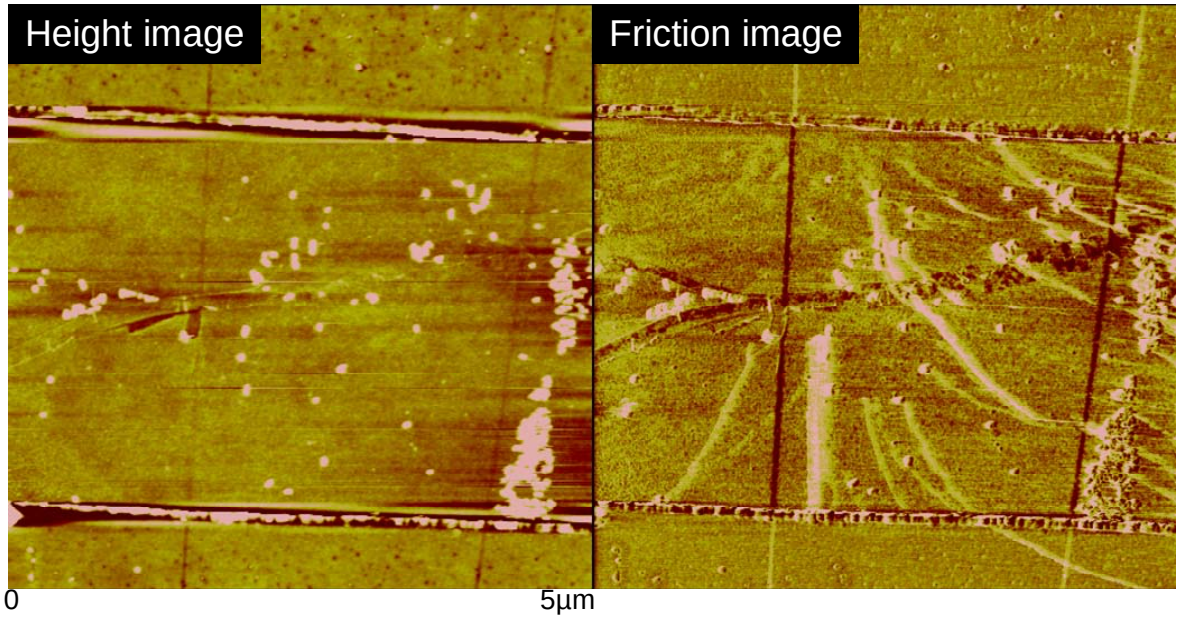

Fig 43: Nanoribbons written in forming gas

Figure 44 shows four different lines, two written in forming gas and two written in nitrogen. The lateral force microscopy signal variation shows that reduction is more complete in forming gas. Furthermore, as the graph in Figure 45 shows, TCNL in forming gas reliably creates ribbons with lower sheet resistances, which means better electrical properties.

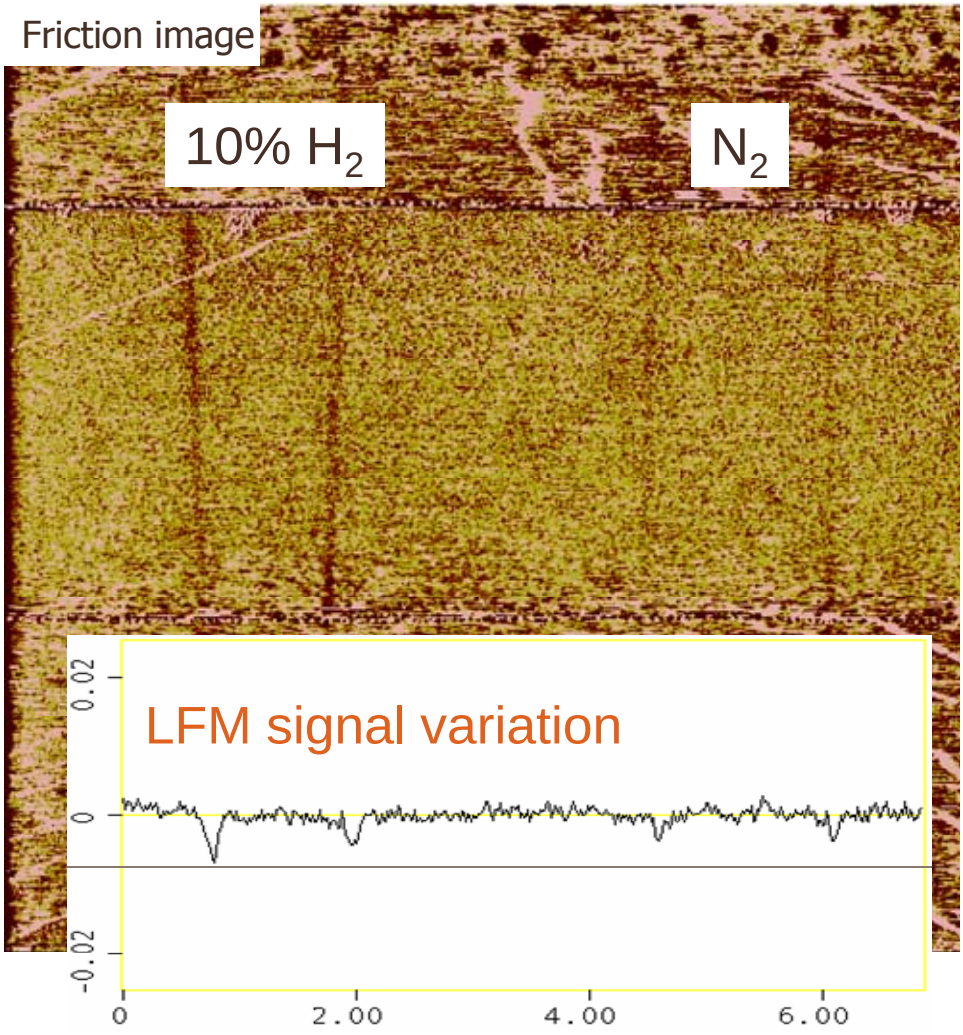

Fig 44: Effect of forming gas on reduction

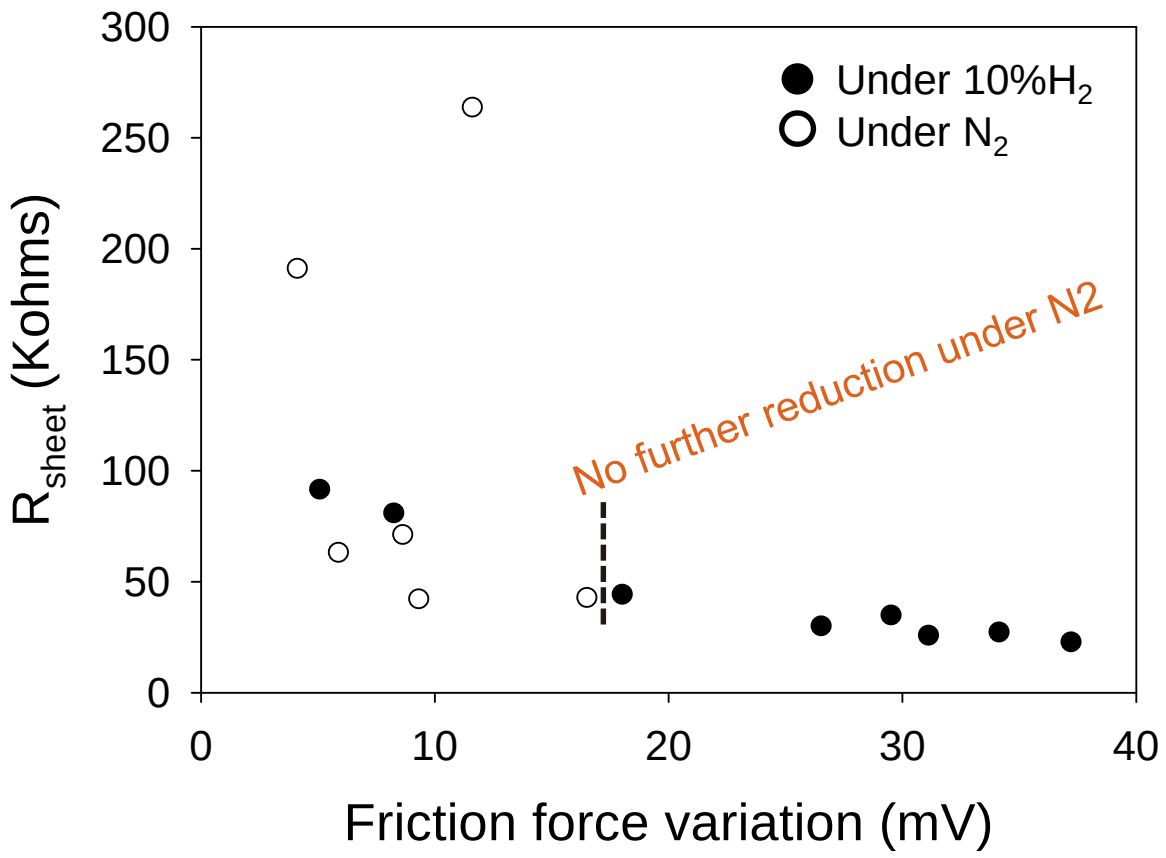

Fig 45: Reduction is more reliable in forming gas

The effect of tip writing speed is also more apparent under forming gas. While under nitrogen increasing the writing speed did not have an appreciable effect on reduction, in forming gas the higher the tip speed resulted in less reduced devices. Figure 46 and 47 show the effect of tip speed on both LFM signal variation and sheet resistance respectively. Namely, in Figure 46, the LFM signal variation is greater, meaning more reduced, for slower speeds. In Figure 47, the sheet resistance is lower, indicating more reduction, for devices written at a slower speed.

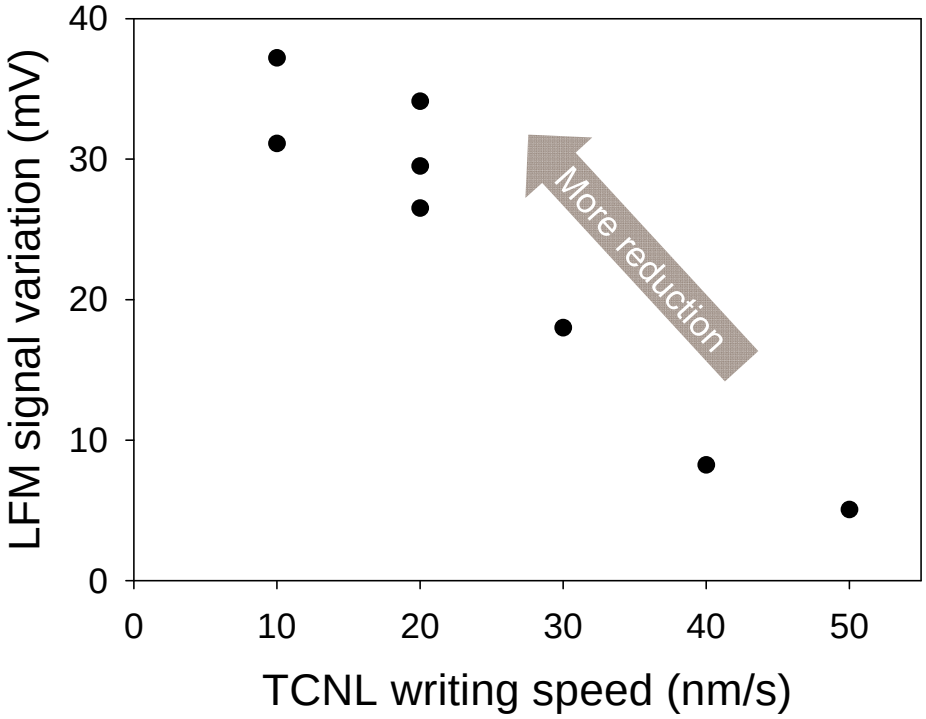

Fig 46: Writing speed vs. LFM signal variation under forming gas

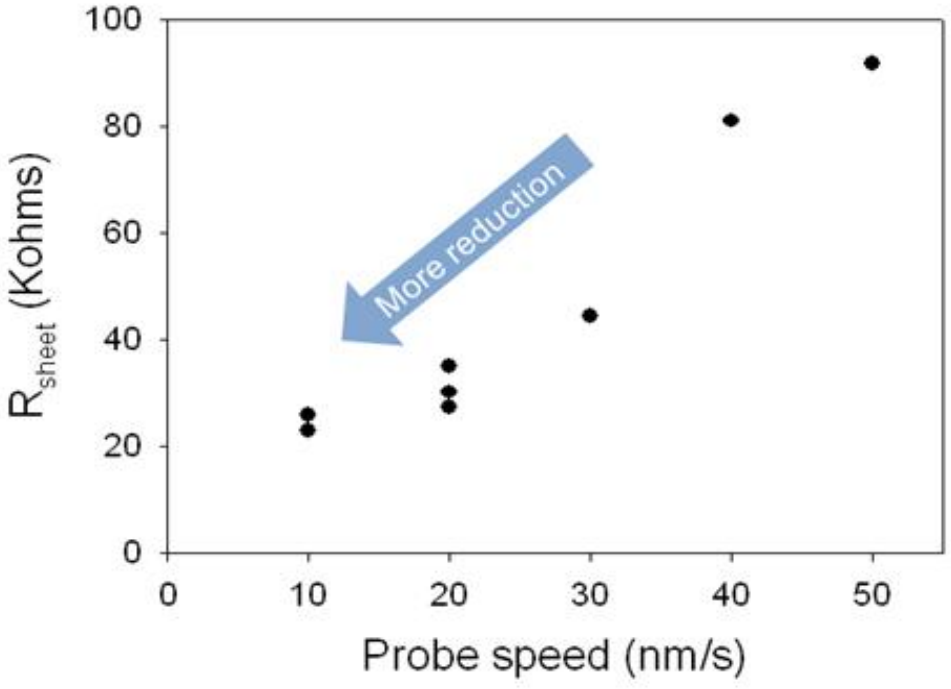

Fig 47: Writing speed vs. device sheet resistance under forming gas

CHAPTER 6: COMPARISON TO OTHER METHODS

Below we compare the properties of the devices we fabricated with properties of graphene-based devices reported in the literature.

6.1 TCNL versus Photolithography

Currently, the process size for photolithography of silicon is 32 nm. This means that the smallest feature size photolithography can industrially produce is 32 nm by 32 nm. Electron beam lithography has gone down to 10 nm in a laboratory setting. Thermochemical nanolithography of fluorographene has continually produced devices that are only three times this size. Furthermore, the hole mobility of silicon is approximately 450 $cm^2 V^{-1} s^{-1}$ [7], which is an order of magnitude above the mobilities of the reduced fluorographene nanoribbons produced throughout this project. We should restate that the values of the mobility depend substantially on the quality of the starting graphene. As the quality of the CVD graphene improves, the mobility of the rFG will improve as well.

6.2 TCNL of Fluorographene versus TCNL of Graphene Oxide

Thermochemical nanolithography has reduced lines into graphene oxide that are 12 nm thick. The lines in the fluorographene were approximately 6 times larger. The nanoribbons produced in graphene oxide and fluorographene had similar electrical properties. The sheet resistance of the TCNL GO was 65 kΩ and that of TCNL FG was 25 kΩ. The primary advantage of the fluorographene version is that it was produced using CVD graphene, which is much easier to work with than is epitaxial graphene, and economically CVD graphene is much more advantageous. Also, the fluorographene was single layer as opposed to multiple layers.

6.3 TCNL versus tDPN

Many techniques cut a graphene sheet into nanoribbons, which introduce negative edge effects. Both TCNL and tDPN write nanoribbons into a larger graphene sheet so that the edge effects are minimized. Direct writing also involves fewer steps than cutting and has the potential to reset the graphene sheet to its initial configuration if so desired by removing all the fluorine and starting over.

The line width and the sheet resistances of devices produced by both thermochemical nanolithography and thermal dip-pen nanolithography are comparable in quality. The mobility of devices produced by tDPN, however, is much higher. This is because the graphene was never rendered insulating before it was chemically isolated. Therefore, the graphene underneath the polymer nano-ribbon deposited by tDPN will be pristine. Compared to the nano-ribbon written into graphene fluoride via TCNL, which may still have residual fluorine, the tDPN device is much cleaner. Unfortunately, tDPN has a few more processing steps and will unlikely achieve less than 20 nm resolution due to the thickness of the polymer.

CHAPTER 7: CONCLUSION

Research on the implementation of graphene in practical technology applications is moving at an extremely fast rate. Currently, there are more than 1000 publications involving CVD graphene, all produced in less than three years. The potential advances that this wonder material can offer are enticing beyond belief.

This Trident project demonstrated a field effect from a graphene nanoribbon transistor produced using atomic force microscopy lithography techniques. This is the first report providing proof-of-concept that graphene transistors (Figure 48) can be directly written into a fluorographene surface. The devices produced throughout this project had sheet resistances comparable to that of previously published results, and other simple improvements to the experimental setup can further improve upon those results.

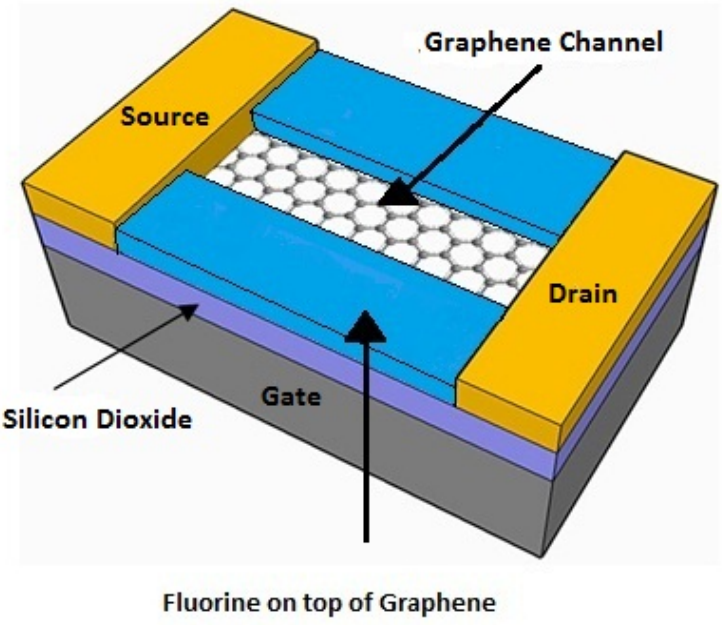

Fig 48: Cartoon image of ideal rFG transistor [27]

Despite the difficulties remaining in order to produce a commercial product from fluorographene, thermochemical nanolithography is an attractive method of manufacturing. TCNL has several advantages over other methods of graphene-based nanoscale transistor fabrication, most important of all being the fewer, safer fabrication steps. There are few intrinsic technological disadvantages to using TCNL or tDPN. The biggest challenge remains the quality of CVD graphene and finding proper ways to transfer the film to the desired substrate.

Applying knowledge to the development of technology has always been seen as a risky venture, but with great risk comes great reward. Furthermore, if no one is willing to risk, then the technology will never advance. This project has provided the first step towards a powerful technique capable to reinvent or create a new avenue for the fabrication of high density electronic devices.

REFERENCES

[1] F. Schwierz, "Graphene Transistors," *Nature Nanotechnology* **5** (2010): 487-496. Reprinted with permission from Macmillan Publishers Ltd: [NATURE NANOTECHNOLOGY] (1) copyright (2010)

[2] K. S. Novoselov, A. K. Geim, S. V. Morozov, D. Jiang, Y. Zhang, S. V. Dubonos, I. V. Grigorieva and A. A. Firsov. "Electric Field Effect in Atomically Thin Carbon Films." *Science* **306** (2004): 666-669.

[3] "Mount graphene to put break on electrons." Available online at http://www.futurity.org/science-technology/mount-graphene-to-put-brake-on-electrons/

[4] C. Lee , X. Wei, J. W. Kysar, and J. Hone. "Measurement of the Elastic Properties and Intrinsic Strength of Monolayer Graphene." *Science* **321** (2008): 385-388.

[5] Sheehan, Paul. "Direct-Write Graphene Nanoribbon Circuitry," Power Point. Naval Research Laboratory, Washington.

[6] Z. Wei, D. Wang, W. de Heer, P. Sheehan, E. Riedo, S. Kim, S.Y. Kim, M. Yakes, A.

Laracuente, Z. Dai, S. Marder, C. Berger, and W. King. "Nanoscale Tunable Reduction of Graphene Oxide for Graphene Electronics." *Science* **328** (2010): 1373-5.

[7] "Silicon electrical Properties," Available online at http://www.ioffe.rssi.ru/SVA/NSM/Semicond/Si/electric.html

[8] M.H Rummeli, C.G Rocha, F. Ortmann, I. Ibrahim, H. Sevincli, F. Borrnert, J. Kunstmann, A. Bachmatiuk, M. Potschke, M. Shiraisji, M. Meyyappan, B. Buchner, S. Roche, G. Cuniberti, "Graphene: piecing it together," Adv. Mat. **23** (2011): 4471-4490.

[9] J.T. Robinson, J.S. Burgess, C.E. Junkermeier, S.C. Badescu, T.L. Reinecke, F.K. Perkins, M.K. Zalalutdniov, J.W. Baldwin, J.C. Culbertson, P.E. Sheehan, and E.S. Snow. "Properties of Fluorinated Graphene Films." Nano Lett. **10** (2010): 3001–3005.

[10] "Fluorographene," Available online at http://fluorographene.org/

[11] "Atomic Force Microscopy." Available online at http://www.nanoscience.com/education/afm.html

[12] "Atomic Force Microscopy." Available online at http://www.qilerongrong.org/Pro_Zhao.html

[13] Booker, Boysen. *Nanotechnology for dummies,* 54.

[14] "Atomic Force Microscopy." Available online at http://www.nanotech-now.com/Art_Gallery/antonio-siber.htm

[15] D. M. Eigler, C. P. Lutz, W. E. Rudge, "An atomic switch realized with the scanning

tunneling microscope," *Nature* **352** (1991): 600-603.

[16] D.J. Walkey. "Physical Electronics: MOSFET Operation." Available online at http://www.doe.carleton.ca/~tjs/21-mosfetop.pdf

[17] "Semiconductor Fabrication: Photolithography," Available online at http://britneyspears.ac/physics/fabrication/photolithography.htm

[18] "Photolithography." Available online at http://www.ece.gatech.edu/research/labs/vc/

[19] W.A. de Heera, C. Bergera, X. Wua, P.N. Firsta, E.H. Conrada, X. Lia, T. Lia, M. Sprinklea, J. Hassa, M.L. Sadowskib, M. Potemskib, G. Martinezb, "Epitaxial Graphene", Solid State Communications **143** (2007): 92-100.

[20] A. Bagri, C. Mattevi, M. Acik, Y.J. Chabal, M. Chhowalla, and V.B. Shenoy, "Structural evolution during the reduction of chemically derived graphene oxide." Nature Chemistry **2** (2010), 581-587.

[21] X. Li, W. Cai, J. An, S. Kim, J. Nah, D. Yang, R. Piner, A. Velamakanni, I. Jung, E. Tutuk, S.K. Banerjee, L. Colombo, R.S. Ruoff, "Large-Area Synthesis of High-Quality and Uniform Graphene Films on Copper Foils", Science **324** (2009): 1312-1314.

[22] W-K. Lee, J.T. Robinson, D. Gunlycke, R.R. Stine, C.R. Tamanaha, W.P. King, and P.E. Sheehan, "Chemically isolated graphene nanoribbons reversibly formed in fluorofraphene using polymer nanwire masks", Nano Lett. **11** (2011): 5461-5464.

[23] H. Conley, "Uniaxially Strained Graphene Resonators." Lecture, March Meeting from American Physical Society, Boston, MA, February 27, 2012.

[24] http://www.ust.hk/spade/introduction/Probe_Station.html

[25] H. Gleskova and S. Wagner, "Electron mobility in amorphous silicon thin-film transistors

under compressive strain," *Applied Physics Letters* **79** (2001):

[26] R.J. Kline and M.D. McGehee, *Adv. Mater.* **15** (2003): 1519.

[27] "Graphene Transistor." Available online at

http://www.livenano.org/technologies/graphene-transistor/

APPENDIX A: STEP-BY-STEP PROCESS

This part will provide step-by-step instructions regarding the AFM reduction process It will begin with an insulating sample of fluorographene fabricated at the Naval Research Laboratory's Institute for Nanoscience. The sample is assumed to be on the atomic force microscope table with the tip engaged and ready to begin imaging a 20 μm by 20 μm square with no x or y offset on the Cypher atomic force microscope (Asylum Research, CA).

1. Press "Frame Up"
2. Wait for scan to show the fluorographene device between the two gold electrodes
3. Zoom in on device with 1 μm of gold electrode left both above and below the device
4. Allow scan to finish and save this image for initial reference
5. Using MicroAngelo lithography software, draw the desired path across the device
6. Press "Do It" and when lithography begins press "Stop Litho"
7. Press "Move tip to Pre-Engage"
8. Turn on current to tip, change current to desired level, zero the photodetector
9. Press "Start tip approach"
10. After tip contacts surface press "Do It"
11. If the Z Voltage display shows the tip is contacting with approximately 70-100 volts, continue reducing. If not, disengage and reengage the tip and adjust setpoint as needed
12. After lithography is complete, press "Move to Pre-engage", turn off current, zero photodetector
13. To see the reduced line, press "Start tip approach" and after contact "Frame up"
14. Wait for scan to complete and save image. If reduction was successful, the nanoribbon should be barely visible in the height image, but clearly visible in the lateral (friction) image